

1 **The contribution of microbial communities in
2 polymetallic nodules to the diversity of the deep-sea
3 microbiome of the Peru Basin (4130 – 4198 meter depth)**

4
5 Massimiliano Molari¹, Felix Janssen^{1,2}, Tobias R. Vonnahme^{1,a}, Frank Wenzhöfer^{1,2}
6 and Antje Boetius^{1,2}

7
8 ¹ Max Planck Institute for Marine Microbiology, Bremen, Germany

9 ² HGF-MPG Joint Research Group on Deep Sea Ecology and Technology, Alfred
10 Wegener Institute for Polar and Marine Research, Bremerhaven, Germany

11
12 ^a Present address: UiT the Arctic University of Tromsø, Tromsø, Norway

13
14 *Correspondence to:* Massimiliano Molari (mamolari@mpi-bremen.de)

16 **Abstract.** Industrial-scale mining of deep-sea polymetallic nodules will remove nodules in large areas
17 of the seafloor. The regrowth of the nodules by metal precipitation is estimated to take millions of
18 years. Thus, for future mining impact studies, it is crucial to understand the role of nodules in shaping
19 microbial diversity and function in deep-sea environments. Here we investigated microbial community
20 composition based on 16S rRNA gene sequences retrieved from sediments and nodules of the Peru
21 Basin (4130 – 4198 m water depth). The nodule field of the Peru Basin showed a typical deep-sea
22 microbiome, with dominance of the classes Gammaproteobacteria, Alphaproteobacteria,
23 Deltaproteobacteria, and Acidimicrobiia. Nodules and sediments host distinct bacterial and archaeal
24 communities, with nodules showing lower diversity and a higher proportion of sequences related to
25 potential metal-cycling bacteria (i.e. Magnetospiraceae, Hyphomicrobiaceae), bacterial and archaeal
26 nitrifiers (i.e. *AqSI*, unclassified Nitrosomonadaceae, *Nitrosopumilus*, *Nitrospina*, *Nitrospira*), and
27 bacterial sequences found in ocean crust, nodules, hydrothermal deposits and sessile fauna. Sediment
28 and nodule communities overall shared a low proportion of Operational Taxonomic Units (OTU; 21 %
29 for Bacteria and 19 % for Archaea). Our results show that nodules represent a specific ecological niche
30 (i.e. hard substrate, high metal concentrations, and sessile fauna), with a potentially relevant role in
31 organic carbon degradation. Differences in nodule community composition (e.g. Mn-cycling bacteria,
32 nitrifiers) between the Clarion-Clipperton Fracture Zone (CCZ) and the Peru Basin suggest that
33 changes in environmental setting (e.g. sedimentation rates) play also a significant role in structuring the
34 nodule microbiome.

35

36 **1 Introduction**

37 Polymetallic nodules (or manganese nodules) occur in abyssal plains (4000–6000 m water depth) and
38 consist primarily of manganese and iron, as well as many other metals and rare earth elements (Crerar
39 and Barnes, 1974; Kuhn et al. 2017). Nodules are potato- or cauliflower-shaped structures with typical
40 diameters of 4–20 cm and are typically found at the sediment surface or occasionally buried in the
41 uppermost 10 cm sediment horizon. The mechanisms of nodule formation are not completely
42 elucidated. The current understanding is that they are formed via mineral precipitations from bottom
43 waters (*Hydrogenetic* growth) or pore waters (*Diagenetic* growth) involving both abiotic and
44 microbiological processes (Crerar and Barnes, 1974; Riemann, 1983; Halbach et al., 1988; Wang et
45 al., 2009). The formation of nodules is a slow process that is estimated to range between thousands and
46 millions of years per millimetre growth (Kerr, 1984; Boltenkov, 2012).

47 Rising global demand for metals has renewed interests in commercial mining of deep-sea nodule
48 deposits. Mining operations would remove nodules, disturb or erode the top decimeters of sediment,
49 and create near bottom sediment plumes that will resettle and cover the seafloor (Miller et al., 2018).
50 Although the first nodules have been discovered in the 1870's (Murray, 1891), only little is known
51 about the biodiversity, biological processes and ecological functions of the nodules and their
52 surrounding sediments as specific deep-sea habitat. Major questions remain, for example as to spatial
53 turnover on local and global scales, the role of the microbial community in and around nodules, and the
54 role of nodules as substrate for endemic species. Hence, there is the need to thoroughly characterize
55 baseline conditions as a requirement for any mining operations as these will require assessments of
56 impacts associated with mining.

57 Extensive and dense nodule fields are found in different areas of the Pacific and Indian Oceans. Nodule
58 accumulations of economic interest have been found in four geographical locations: the Clarion-
59 Clipperton Fracture Zone (CCZ) and the Penrhyn Basin in the central north and south Pacific Ocean,
60 respectively; the Peru Basin in the south-east Pacific; and in the center of the northern Indian Ocean
61 (Miller et al., 2018). To our knowledge the Peru basin is the only region that does not have exploration
62 activities and plans for mining so far. Previous work on the structure of microbial communities of
63 nodule fields by 16S rRNA gene sequencing focused on the CCZ and the central South Pacific Ocean
64 (Xu et al., 2007; Wu et al., 2013; Tully and Heidelberg, 2013; Blöthe et al., 2015; Shulse et al., 2016;
65 Lindh et al., 2017). All studies showed that polymetallic nodules harbour microorganisms that are
66 distinct from the surrounding sediments and overlying water. They indicate that nodule communities
67 show a pronounced spatial variability, but these results are so far not conclusive. Similar microbial
68 communities were observed in nodules collected at distances of 6000 km and 30 km (Wu et al., 2013;
69 Shulse et al. 2016), while Tully and Heidelberg (2013) found that nodule communities varied among
70 sampling sites (<50 km). Besides, potential Mn-oxidizers and -reducers such as *Alteromonas*,
71 *Pseudoalteromonas*, *Shewanella* and *Colwellia* were proposed as a core of the nodule microbiome
72 involved in the formation of nodules (Wu et al. 2013; Blöthe et al., 2015), but they were not found in
73 all nodules sampled so far (Tully and Heidelberg, 2013; Shulse et al. 2016). The lack of knowledge on
74 the diversity and composition of microbial assemblages of other nodule provinces makes it difficult to

75 assess whether observed differences within the CCZ may reflect regional differences in environmental
76 conditions (e.g. input of organic matter, bathymetry, topography, sediment type), or in abundance and
77 morphology of nodules, or in the colonization of the nodules by epifauna and protozoans.

78 In this study we investigated the diversity and composition of bacterial and archaeal communities
79 associated with manganese nodule fields of the Peru Basin. The Peru Basin is located about 3000 km
80 off the coast of Peru and covers about half of the size of the CCZ, which is 5000–9000 km away. The
81 present-day organic carbon flux in this area is approximately two times higher than in the CCZ,
82 resulting in higher content of organic carbon in the surface sediments (>1 % vs 0.2–0.6 % in the CCZ),
83 and a shallower oxic-suboxic front (10 cm vs tens of meters sediments depth in the CCZ; Müller et al.,
84 1988; Heackel et al., 2001; Volz et al., 2018). As a consequence of differences in environmental
85 conditions (e.g. organic carbon flux, carbonate compensation depth, sediment type, topography and
86 near-bottom currents), the Peru basin and the CCZ host manganese nodules with different geological
87 features (Kuhn et al. 2017). This includes: i) nodules from the Peru Basin are often larger, with a
88 typical cauliflower shape, compared to those in CCZ that have a discoidal shape and a size of 2–8 cm
89 (Kuhn et al. 2017); ii) average nodule abundance in the Peru Basin is lower (10 kg m⁻²) than in CCZ
90 (15 kg m⁻²; Kuhn et al. 2017); iii) Mn nodules from the Peru Basin are thought to be mainly formed by
91 suboxic diagenesis, whereas CCZ nodules apparently exhibit a mixture of diagenetic and hydrogenetic
92 origin (von Stackelberg 1997; Chester and Jickells 2012); iv) while Peru Basin and CCZ nodules
93 consist of the same type of mineral (disordered phyllosilicates), they have a different metal content
94 (Wegorzewski and Kuhn 2014; Wegorzewski et al. 2015).

95 An increasing number of studies and policy discussions address the scientific basis of ecological
96 monitoring in deep-sea mining, highlighting the need to identify appropriate indicators and standards
97 for environmental impact assessments and ecological management. A key aspect is avoiding harmful
98 effects to the marine environment, which will have to include loss of species and ecosystem functions.
99 The primary aims of this study were to assess the structure and similarity of benthic microbial
100 communities of nodules and sediments of the Peru Basin nodule province, and to compare them with
101 those of other global deep-sea sediments and nodules in the CCZ. The focus was on similarity
102 comparisons in order to investigate endemism and potential functional taxa that could be lost due to the
103 removal of manganese nodules by mining activities. To achieve this, the hypervariable 16S rRNA gene
104 regions V3-V4 for Bacteria and, V3-V5 for Archaea were amplified from DNA extracted from nodules
105 and surrounding sediments and sequenced using the Illumina paired-end MiSeq platform. The
106 hypotheses tested were i) nodules shape deep-sea microbial diversity, ii) nodules host a specific
107 microbial community compared to the surrounding sediments. Secondary aim of this study was to
108 investigate the nodule features that may play a major role in shaping microbial community composition
109 and microbially-mediated functions.

110

111 **2 Methods**

112 **2.1 Sample collection**

113 Sediment samples and polymetallic nodules were collected as a part of the MiningImpact project of the
114 Joint Programming Initiative JPI Healthy and Productive Seas and Oceans (JPI Ocean) on board of
115 R/V Sonne (expedition SO242/2; 28th of August - 1st of October 2015) in the Peru Basin around 7° S
116 and 88.5° W. Samples were collected at three sites outside the seafloor area selected in 1989 for a long-
117 term disturbance and recolonization experiment (DISCOL; Thiel et al., 2001), for this reason they were
118 called “Reference Sites”: Reference East, Reference West, and Reference South. Sediment samples
119 were collected using TV-guided MULTiple Corer (TV-MUC) at three stations per site (Table 1). The
120 cores were sliced on board in a temperature-controlled room (set at *in situ* temperature), and aliquots of
121 sediment were stored at -20 °C for DNA extraction. Manganese nodules where sampled, using a TV-
122 MUC, or a Remotely Operated Vehicle (ROV KIEL6000, GEOMAR, Germany): one nodule at
123 Reference West and four nodules at Reference South. The nodules were partly located at the surface or
124 buried down to 3 cm below the seafloor (bsf) with diameters of a few cm. Nodules were gently rinsed
125 with 0.22-µm filtered cold bottom seawater to remove adhering sediment, stored in sterile plastic bags
126 at -20 °C and crushed before DNA extraction in the home lab. From the nodules collected with the
127 ROV, only the surface layer was scraped off using a sterile spoon, and subsequently crushed and frozen
128 (-20 °C). Sedimentary metadata (e.g. cell counts, pigments and organic carbon content, porewater
129 profiles, and porosity) and a map of the study area are available in Vonnahme et al. (in press). Focusing
130 entirely on sediments, that publication also includes a discussion of the variability of environmental
131 settings and microbial communities.

132 **2.2 DNA extraction and sequencing**

133 The DNA was extracted from 1 g of wet sediment (0-1 cm layer) and from 1 g of wet nodule's
134 fragments using the FastDNATM SPIN Kit for Soil (Q-BIOgene, Heidelberg, Germany) following the
135 protocol provided by the manufacturer. An isopropanol precipitation was performed on the extracted
136 DNA, and DNA samples were stored at -20 °C. As control for DNA contamination (negative control),
137 DNA extraction was carried out on purified water after being in contact with sterile scalpel and plastic
138 bag.

139 Amplicon sequencing was done at the CeBiTec laboratory (Centrum für Biotechnologie, Universität
140 Bielefeld) on an Illumina MiSeq machine. For the 16S rRNA gene amplicon library preparation we
141 used the bacterial primers 341F (5'-CCTACGGNGGCWGCAG-3') and 785R (5'-
142 GACTACHVGGTATC TAATCC-3'), and the archaeal primers Arch349F (5'-
143 GYGCASCAGKCGMGAAC-3') and Arch915R (5'-GTGCTCCCCGCCAATTCT-3') (Wang and
144 Qian, 2009; Klindworth et al., 2013), which amplify the 16S rRNA gene hypervariable region V3-V4
145 in Bacteria (400–425 bp fragment length) and the V3-V5 region in Archaea (510 bp fragment length).
146 The amplicon library was sequenced with the MiSeq v3 chemistry, in a 2x300 bp paired run with
147 >50,000 reads per sample, following the standard instructions of the 16S rRNA gene Metagenomic
148 Sequencing Library Preparation protocol (Illumina, Inc., San Diego, CA, USA).

149 The quality cleaning of the sequences was performed with several software tools. CUTADAPT
150 (Martin, 2011) was used for primer clipping. Subsequently the TRIMOMATIC software (Bolger et
151 al., 2014) was used to remove low-quality sequences starting with the following settings:
152 SLIDINGWINDOW:4:10 MINLEN:300 (for Bacteria); SLIDINGWINDOW:6:13 MINLEN:450 (for
153 Archaea). In case of bacteria data this step was performed before the merging of reverse and forward
154 reads with PEAR (Zhang et al., 2014). Low-quality archaeal sequences were removed after merging
155 the reads in order to enhance the number of retained reads due to the increase in archaeal 16S rRNA
156 gene fragment length. All sequences were quality controlled with FastQC (Andrews, 2010). Where
157 necessary, more sequences were removed with TRIMOMATIC with larger sliding window scores
158 until the FastQC quality control was passed (average quality score per sample >34 for Bacteria and >22
159 for Archaea). Clustering of sequences into OTUs (operational taxonomic units) was done using the
160 SWARM algorithm (Mahé et al., 2014). The taxonomic classification was based on the SILVA rRNA
161 reference database (release 132), at a minimum alignment similarity of 0.9, and a last common ancestor
162 consensus of 0.7 (Pruesse et al., 2012). Workflow and scripts applied in this study can be found in
163 Hassenrück et al. (2016). Raw sequences with removed primer sequences were deposited at the
164 European Nucleotide Archive (ENA) under accession number PRJEB30517 and PRJEB32680; the
165 sequences were archived using the service of the German Federation for Biological Data (GFBio;
166 Diepenbroek et al., 2014).

167 The total number of sequences obtained in this study is reported in Table S1. Absolute singletons
168 (SSOabs), i.e. OTUs consisting of sequences occurring only once in the full dataset (Gobet et al., 2013)
169 were removed (Table S1). Similarly, contaminant sequences (as observed in the negative control) and
170 unspecific sequences (i.e., bacterial sequences in the archaeal amplicon dataset, and archaeal,
171 chloroplast, and mitochondrial sequences in the bacterial dataset) were removed from amplicon data
172 sets before the analysis (Table S1). The dominant OTU sequences and OTU sequences highly abundant
173 in the nodules were subjected to BLAST search (BLASTn; GeneBank nucleotide database 12/06/2019;
174 Altschul et al., 1990) in order to identify in which others habitats the closest related (i.e. >99 %)
175 sequences have been previously reported.

176 2.3 Data analysis

177 The first three Hill Numbers, or the effective number of species, were used to describe alpha-diversity:
178 species richness (H_0), the exponential of Shannon entropy (H_1), and the inverse Simpson index (H_2 ;
179 Chao et al., 2014). Coverage-based and sample-size-based rarefaction (based on actual number of
180 sequences) and extrapolation (based on double number of sequences) curves were calculated for the
181 Hill's numbers using the R package iNEXT (Hsieh et al., 2018). Calculation of the estimated richness
182 (Chao1) and the identification of unique OTUs (present exclusively in one sample) were based on
183 repeated ($n = 100$) random subsampling of the amplicon data sets. Significant differences in alpha-
184 diversity indices between substrates (i.e. manganese nodules and sediments) were determined by
185 analysis of variance (ANOVA), or by non-parametric Kruskal-Wallis test (KW) when ANOVA's
186 assumptions were not satisfied.

187 Beta-diversity in samples from different substrates and from different sites was quantified by
188 calculating an Euclidean distance matrix based on centred log-ratio (CLR) transformed OTU
189 abundances (function *clr* in R package *compositions*) and Jaccard dissimilarity based on a
190 presence/absence OTU table. The latter was calculated with 100 sequence re-samplings per sample on
191 the smallest dataset (40613 sequences for Bacteria and 1835 sequences for Archaea). Euclidean
192 distance was used to produce non-metric multidimensional scaling (NMDS) plots. The Jaccard
193 dissimilarity coefficient was used to perform hierarchical clustering (function *hclust* in R package
194 *vegan*, using the complete linkage method), and the dissimilarity values for cluster nodes were used to
195 calculate the number of shared OTUs between/within groups. The permutational multivariate analysis
196 of variance (PERMANOVA; Anderson, 2001) was used to test difference in community structure and
197 composition.

198 Differentially abundant OTUs and genera were detected using the R package ALDEx2 (Fernandes et
199 al. 2014) at a significance threshold of 0.01 and 0.05 for Benjamini–Hochberg (BH) adjusted
200 parametric and non-parametric (KW) P-values, respectively. We only discuss the taxa that were at least
201 two times more abundant in nodules than in sediments (i.e. $\text{Log2}(\text{Nodule}/\text{sediment}) \geq 1$) and with a
202 sequences contribution of total number of sequences $\geq 1\%$ (for genera) or $\geq 0.1\%$ (for OTUs).
203 All statistical analyses were conducted in R using the core distribution with the additional packages
204 *vegan* (Oksanen et al. 2015), *compositions* (Van den Boogaart et al., 2014), *iNEXT* (Hsieh et al.,
205 2018), and *ALDEx2* (Fernandes et al. 2014).

206 3 Results

207 3.1 Microbial alpha-diversity

208 Bacterial and archaeal communities in 5 nodules and 9 sediment samples (Table 1) were investigated
209 using specific sets of primers for Bacteria and Archaea on the same extracted pool of DNA per station.
210 The number of bacterial sequences retrieved from DNA extracted from sediments and nodules was on
211 average 5 ± 5 and 25 ± 14 times higher, respectively, than those obtained for archaea (t-test: $p < 0.001$,
212 $df = 11$, $t = 4.5$).

213 Table S1 shows the statistics of sequence abundance and proportion of singletons and cosmopolitan
214 types. Sequence abundances of bacteria were comparable between sediments and nodules.
215 Cosmopolitan OTU, i.e. those present in 80 % of the sediments and nodule samples, were only 9 % of
216 all taxa (77 % of all sequences), whereas rare OTUs occurring only in <20 % of all samples
217 represented 50 % the taxa (4 % of all sequences). Sediments vs nodules contained only 4 and 2 %,
218 respectively, of endemic taxa, defined as those were abundant in either substrate but rare in the other.
219 Thus the contribution of unique OTUs to the total number of OTUs was lower in manganese nodules
220 than in sediments samples (Table 2, Figure 1a). Bacterial and archaeal diversity was investigated
221 calculating the total number of OTUs (Hill number $q=0$; H_0) and the estimated richness (Chao1), and
222 the unique OTUs (present exclusively in one station). For this analysis, the latter were calculated with
223 sequence re-sampling, to overcome differences in sequencing depth. Abundance-based coverage
224 estimators, exponential Shannon (Hill number $q=1$; H_1) and inverse Simpson (Hill number $q=2$; H_2),

were also calculated. The rarefaction curve indicates that the richness (H_0) of the less abundant and rare OTUs was somewhat underestimated both in nodules and in sediments (Figure S1 a-b). However, the bacterial and archaeal diversity was well described for the abundant OTUs (H_1 and H_2 ; Figure S1 a-b); with more than 90 % of the estimated diversity covered (Figure S1 c-d). Both in sediments and nodules the alpha-diversity indices were higher for Bacteria than for Archaea (t-test: $p<0.0001$, $df=12$, $t=8.0-16.0$), while the contribution of unique OTUs to the total number of OTUs was comparable (Table 2). Bacterial communities in manganese nodules have lower Hill numbers and Chao1 indices compared to those associated to sediments (Table 2, Figure 1a). Archaeal communities showed the same patterns for diversity indices and unique OTUs, with exception for the H_2 index that did not show significant difference between nodules and sediments (Table 2, Figure 1b).

3.2 Patterns in microbial community composition

The changes in microbial community structure at OTU level (beta-diversity) between substrates and samples were quantified by calculating Euclidean distances from CLR transformed OTU abundance. Shared OTUs were estimated by calculating Jaccard dissimilarity from OTU presence/absence based on repeated random subsampling of the amplicon data sets. Microbial communities associated with manganese nodules differed significantly from those found in the sediments (Figure 2, Table S2). Also, significant differences were detected in sediment microbial community structure among the different sites (PERMANOVA; Bacteria: $R^2 = 0.384$; $p = 0.003$; $F_{2,8} = 1.87$; Archaea: $R^2 = 0.480$; $p = 0.013$; $F_{2,8} = 2.31$; Table S2), and between communities associated with nodules and sediment at Reference South site (PERMANOVA; Bacteria: $R^2 = 0.341$; $p = 0.023$; $F_{1,6} = 2.59$; Archaea: $R^2 = 0.601$; $p = 0.029$; $F_{1,6} = 7.53$; Table S2), which was the only site where the number of samples allowed for the test. “Site” defined by geographic location, and “Substrate”, i.e. origin from sediment or nodule, explained a similar proportion of variation in bacterial community structure (27 % and 23 %, respectively). “Substrate” had a more important role in shaping archaeal communities than “Site” (explained variance 35 % and 19 %, respectively; Table S2). The number of shared OTUs between nodules and sediments (Bacteria: 21 %; Archaea: 19 %) was lower than those shared within nodules (Bacteria: 30 %; Archaea: 30 %) and within sediments (Bacteria: 31 %; Archaea: 32 %) (Figure S2).

Bacterial communities in manganese nodules and sediments were dominated by the classes Gammaproteobacteria (26 %), Alphaproteobacteria (19 %), Deltaproteobacteria (9 %), Bacteroidia (5 %), Acidimicrobia (4 %), Dehalococcoidia (4 %), Planctomycetacia (4 %), Nitrospinia (3 %), and Phycisphaerae (3 %), which accounted for more than 75 % of the total sequences (Figure 3). All archaeal communities were dominated by Thaumarchaeota (*Nitrosopumilales*), which represented more than 95% of all sequences. The remaining small proportion of sequences was taxonomically assigned to *Woesearchaeia* (Figure S2b). Nodule and sediment samples showed similar compositions of most abundant bacterial genera (contribution to total number of sequence ≥ 1 %; Figure S2a). 69 bacterial genera (9 % of all genera) were differentially abundant in the nodules and in the sediment, accounting for 36 % and 21 % of total sequences retrieved from nodules and sediments, respectively (ALDEx2: ANOVA adjusted $p<0.01$ and KW adjusted $p<0.05$; Figure 4 and Table S3). Of those only one unclassified genus within the family of Sphingomonadaceae and the genus *Filomicrombium* were

264 exclusively found in nodules and not in the sediment samples, and their contribution to the total
265 number of sequences was less than 0.06 %. Genera that were more abundant in the nodules than in the
266 sediments included: unclassified Alphaproteobacteria (7 %), *Nitrospina* (4 %), unclassified SAR324
267 clade (Marine group B; 3 %), unclassified Hyphomicrobiaceae (3 %), Pirellulaceae Pir4 lineage (2 %),
268 unclassified Methyloligellaceae (1 %), unclassified Pirellulaceae (1 %), *Acidobacteria*, unclassified
269 Subgroup 9 (1 %) and Subgroup 17 (1 %), Nitrosococcaceae *AqSI* (1 %), Calditrichaceae *JdFR-76* (1
270 %), and *Cohesibacter* (1 %) (Figure 4 and Table S3). In the sediment we identified 21 genera that
271 were more abundant than in the nodules, but all together they represented only 3 % of total sequences
272 recovered from sediments. 128 OTUs were highly abundant in nodules (ALDEx2: ANOVA adjusted
273 p<0.01 and KW adjusted p<0.05), which accounts for 24 % of total sequences retrieved from nodules
274 (Table 3a). The closest related sequences ($\geq 99\%$ similarity) were retrieved from ocean crusts (30 %),
275 from nodule fields (26 %), from hydrothermal/seep sediments and deposits (21 %), from worldwide
276 deep-sea sediments (16 %), and associated to invertebrates (7 %; Table 3b and Figure 5).

277 4 Discussion

278 Industrial-scale mining of deep-sea polymetallic nodules may remove nodules and the active surface
279 seafloor layer at a spatial scale ranging from ca. 50000–75000 km² per claim to ca. 1 million km²
280 including all current exploration licences (Miller et al., 2018). The regrowth of nodules will take
281 millions of years, thus it is unknown if the associated biota could recover at all (Simon-Lledo et al.,
282 2019). The response of microbial communities to the loss of nodules and seafloor integrity is largely
283 unknown. It may play an important role in the ecological state of the seafloor habitat due to the many
284 functions bacteria and archaea hold in the food-web, element recycling, and biotic interactions, beyond
285 representing the largest biomass in deep-sea sediments (Joergensen and Boetius 2007). It is thus crucial
286 to understand the role of nodules in shaping microbial diversity and in hosting microbes with important
287 ecological functions. So far, only few studies were carried out to investigate the microbiota of nodule
288 fields, and most of them were focused on identifying microbes involved in metal cycling. Here, we
289 investigated similarity of microbial community structures in sediments and nodules retrieved from the
290 Peru Basin. The objectives of this study were: i) compares the microbes of nodule fields with
291 microbiota of deep-sea sediments, in order to identify specific features of microbial diversity of nodule
292 fields; ii) elucidates differences in diversity and in microbial community structure between sediments
293 and nodules; iii) investigates potential microbially-mediated functions and the major drivers in shaping
294 microbial communities associated to the nodules.

295 4.1 Microbial diversity of nodule fields is distinct from other deep-sea areas

296 Benthic bacterial assemblages in sediments and nodules of the Peru basin showed the typical
297 dominance of the classes Gammaproteobacteria, Alphaproteobacteria, Deltaproteobacteria, and
298 Acidimicrobiia, as reported for deep-sea sediments worldwide (Bienhold et al., 2016; Figure 3) and in
299 the Pacific Nodule Province (Wang et al., 2010; Wu et al., 2013; Shulse et al., 2016; Lindh et al.,
300 2017). However at higher taxonomic resolution we detected substantial differences to the microbial

301 community composition of other deep-sea regions. Sediments of the Peru Basin bacteria classes were
302 depleted in sequence abundances of Flavobacteria, Gemmatimonadetes and Bacilli, whereas sequence
303 abundances of the Chloroflexi (i.e. Dehalococcoidia), Planctomycetes (i.e. Pirellulaceae,
304 Phycisphaeraceae) and the genus *Nitrospina* were higher compared to other deep-sea regions (Bienhold
305 et al., 2016, Varliero et al., 2019). Dehalococcoidia and Planctomycetes were previously reported as
306 important component of benthic microbial assemblages in the Pacific Ocean (Wang et al., 2010; Wu et
307 al., 2013; Blöthe et al., 2015; Walsh et al., 2016; Lindh et al., 2017). Their contribution to the total
308 community was found to increase in organic matter depleted subsurface sediments (Durbin and Teske,
309 2011; Walsh et al., 2016).

310
311 Dominant OTUs (>1 %) belonged to unclassified Actinomarinales, Gammaproteobacteria, Subgroup
312 21 (phylum Acidobacteria), and to genus *Woesia* (family Woeseiaceae). Members of Actinomarinales
313 and Woeseiaceae are cosmopolitan types in deep-sea sediments (Bienhold et al., 2016). For
314 Actinomarinales there are no cultured relatives, and the function of this group remains unknown. In the
315 case of Woeseiaceae, one representative is in culture (*Woeseia ocaeni*). *W. ocaeni* is an obligate
316 chemoorganoheterotroph (Du et al., 2016), suggesting a role in organic carbon remineralization for
317 members of that family, as recently confirmed by analysis of deep-sea assembled genomes (Hoffmann
318 et al., 2020). Closest related sequences of Subgroup 21 have been reported in deep-sea sediments
319 (Schauer et al. 2010) and across Pacific nodule fields (Wu et al., 2013), but also in association with
320 deep-sea benthic giant foraminifera (Xenophyophores) and in surrounding sediments (Hori et al.,
321 2013). The subgroup 21-like OTU was also one of the 10 most abundant OTUs retrieved from nodules
322 (0.9 %). Xenophyophores have agglutinated tests and can grow to decimetre size, suggesting that
323 members of Subgroup 21 may be colonists of biological and/or hard substrates.

324
325 Within the class Alphaproteobacteria the most abundant OTUs (>0.5 %) belonged to unclassified
326 genera of the families Magnetospiraceae (order Rhodospirillales), Hyphomicrobiaceae (order
327 Rhizobiales), and Kiloniellaceae (order Rhodovibrionales). Magnetospiraceae and Hyphomicrobiaceae
328 are the most abundant families in nodules with >2 % of OTUs. Closely related sequences have been
329 reported previously across Pacific Nodule Provinces (Xu et al., 2007; Shulse et al., 2016). The family
330 of Magnetospiraceae includes microaerophilic heterotrophs, able of magnetotaxis and iron reduction
331 (i.e. genus *Magnetospirillum*; Matsunaga et al. 1991; Schuler and Frankel, 1999), and thus the
332 members of this family could play a role in Fe(III) mobilization, affecting its bioavailability.
333 Hyphomicrobiaceae-like sequences found in this study are related to genera *Hyphomicrobium* and
334 *Pedomicrobium* (sequence identity 97 %), which have been reported to be involved in manganese
335 cycling (Tyler, 1970; Larsen et al., 1999; Stein et al., 2001). A potential contribution of these groups in
336 metal cycling in manganese nodules is also suggested by the presence of closest related sequences in
337 ocean crust (Santelli et al., 2008; Lee et al., 2015), which typically hosts epilithic and endolithic
338 microbial communities of chemolithotrophic metals-oxidizers (Staudigel et al., 2008). Similarly,
339 Kiloniellaceae related OTUs might be involved in metal-cycling as closely related sequences were
340 found in marine basalts (Mason et al., 2007; Santelli et al., 2008) and inside other manganese nodules

341 (Blöthe et al., 2015). Most of the marine cultivates in the family Kiloniellaceae belong to genus
342 *Kiloniella*, that have been isolated from marine macroalga (Wiese et al., 2009), the guts of Pacific
343 white shrimp (Wang et al., 2015), marine sponge (Yang et al., 2015), spider crab and clam (Gerpe et
344 al., 2017), and from the surface water of a polynia in the Western Antarctic Sea (Si et al., 2017).
345 Besides, Kiloniellaceae-like sequences were found in sponges (Cleary et al., 2013), sea star larvae
346 (Galac et al., 2016) and in seamount's iron mats (Scott et al., 2017). The presence of rich sessile and
347 mobile metazoan communities associated to nodules offers various potential hosts for members of
348 Kiloniellaceae. *Kiloniella* is a chemoheterotrophic aerobe, and the draft genome of an isolate from the
349 gut of a Pacific white shrimp shows potential for denitrification and iron acquisition and metabolism
350 (Wang et al., 2015). Thus, either as free-living or host-associated life, the potential contribution of
351 Kiloniellaceae in metal cycling requires further investigation.

352

353 Archaea were also present in sediments of the Peru Basin, with Nitrosopumilaceae (phylum
354 Thaumarchaeota) dominating the archaeal communities (Figure S2b). Archaeal sequences comprised a
355 lower portion of total sequences retrieved from sediments (6 – 45 %) and nodules (<1 – 7 %) of Peru
356 basin, and they were lower in nodules compared to the sediments. Our data differed from what was
357 reported by Shulse et al. (2016) for CCZ, especially for nodules (ca. 20%). We cannot rule out that the
358 observed differences in microbial community structure partly reflect the different sets of primers used
359 in our study and by Shulse et al. (2016). As both primer sets amplified the same hypervariable region
360 of 16S rRNA gene (V4) we assume that biases are small enough to justify the comparison. The
361 majority of member of Nitrosopumilaceae are believed to be capable of oxidation of ammonia to
362 nitrite, the first step of nitrification (Offre et al., 2013). Archaeal ammonia oxidizers have a higher
363 affinity for ammonia than bacterial ammonia oxidizers, and they are favoured in environments with
364 low ammonia concentrations (Martens-Habbena et al., 2009). The Peru Basin has higher particulate
365 organic-carbon fluxes as compared to central Pacific Ocean (Haeckel et al., 2001; Mewes et al., 2014),
366 which results in higher remineralisation rates and higher ammonia fluxes. These limit the thickness of
367 oxygenated sediments to 10 cm in the Peru Basin while they can reach up to 2-3 m depth in the CCZ
368 (Haeckel et al., 2001; Mewes et al., 2014; Volz et al., 2018). Hence differences observed between CCZ
369 and Peru nodule fields in the contribution of archaeal sequences to microbial assemblages are likely
370 due to ammonia availability, which is controlled by organic matter fluxes.

371 **4.2 Microbial community structure differs between sediments and nodules**

372 Beta-diversity of microbial community structure in the Peru Basin sediments showed remarkable
373 spatial OTU turnover already on a local scale (<60 km; Figure S2), which is at the higher end of
374 previous microbial beta-diversity estimates for bathyal and abyssal seafloor assemblages (Jacob et al.,
375 2013; Ruff et al., 2015; Bienhold et al., 2016; Walsh et al., 2016; Varliero et al., 2019). Here we
376 focused specifically on the contribution of nodules to diversity, which could be a critical parameter in
377 the ecological assessment of nodule removal. Analysis of community composition at OTU level shows
378 that nodules and sediments host distinct bacterial and archaeal communities (Figure 2), as previously
379 reported also for CCZ (Wu et al., 2013; Tully and Heidelberg, 2013; Shulse et al., 2016; Lindh et al.

380 2017). Albeit the microbial communities in the sediment showed significant differences between sites,
381 the low number of shared OTUs between sediments and nodules <20 % supports the presence of
382 specific bacterial and archaeal communities associated with polymetallic nodule habitats. However, the
383 proportion of truly endemic, unique nodule OTUs was also low (Figure 1a, Table S1), nonetheless it is
384 relevant to highlight that nodule removal would lead to a loss of specific types of microbes in a mined
385 deep-sea region (Blöthe et al., 2015).

386 Microbial communities associated with nodules are significantly less diverse than those in the
387 sediments, and the decrease in diversity was observed both in rare and abundant bacterial types (Figure
388 1 and Figure S1). This seems to be a common feature of polymetallic nodules (Wu et al., 2013; Tully
389 and Heidelberg, 2013; Zhang et al., 2014; Shulse et al., 2016; Lindh et al. 2017). However, a recent
390 meta-analysis of 16S rRNA gene diversity reports no significant differences in microbial biodiversity
391 between nodules and sediments within the studied habitats in the CCZ (Church et al., 2019). Church
392 and colleagues also pointed out that the findings are so far not conclusive due to the limited number of
393 studies and differences in methods (e.g. PCR primers, sequencing approaches), which may also be a
394 reason for the differences between the meta-analysis and the results of this study. Tully and Heidelberg
395 (2013) suggested that lower microbial diversity in the nodules might be due to less availability of
396 potential energy sources (e.g. organic matter) compared to sediments. Despite that the sedimentation
397 rate exceeds the growth rate of nodules, the nodules are typically exposed to bottom water and not
398 covered by sediments (Peukert et al., 2018). Although, it is unknown whether physical mechanisms
399 (e.g. current regime or seasonal events) or biological processes (e.g. grazing, active cleaning) are
400 responsible for lack of sediments accumulation on nodules, the decrease of microbial diversity with the
401 decrease of organic matter availability is in accordance with positive energy-diversity relationship
402 reported for deep-sea sediments (Bienhold et al., 2012). However, the presence of foraminiferal
403 assemblages (Gooday et al., 2015) and specific sessile metazoan communities (Vanreusel et al., 2016)
404 on the surface of nodules may represent a potential source of transformed organic matter (e.g.
405 dissolved organic matter) and catabolic products, which may represent a much more valuable energy
406 source for microbes than refractory particulate organic matter sinking from the water column.
407 Furthermore, higher microbial diversity in the sediments than in the nodules could be the result of the
408 accumulation of allochthonous microbes, as suggested by the higher proportion of rare and unique
409 OTUs in the sediments. Lastly, the nodules offer hard substrate and presence of metals, which can
410 select for specific Bacteria and Archaea. Similarly, hydrothermal deposits have typically lower
411 bacterial diversity than deep-sea sediments despite chemical energy sources being highly available
412 (Ruff et al., 2015; Wang et al., 2018). We propose that the decreased diversity of abundant OTUs in
413 nodules, observed especially for Bacteria, suggests selection for colonists adapted to specific ecological
414 niches associated with nodules (e.g. high metals concentration, hard substrate, presence of sessile
415 fauna).

416 **4.3 Potential functions of microbial communities associated to nodules**

417 The presence of a large proportion of bacterial community with low abundance in the sediments, but
418 enriched in the nodules both at the level of genera (35 %) and OTUs (24 %) (Figure 4, Table S3 and

419 Table 3a) indicates niche specialization. The most abundant OTUs (13 % of the bacterial community)
420 in nodules include unclassified Hyphomicrobiaceae, Magnetospiraceae, Alphaproteobacteria,
421 Arenicellaceae and SAR324, *Nitrospina*, *AqSI*, Methyloligellaceae, Subgroup 9, Subgroup 17,
422 Kiloniellaceae, *Cohaesibacter* and JdFR-76, which closest related sequences have been retrieved from
423 Pacific nodules (e.g. Wu et al. 2013; Blöthe et al., 2015), basaltic rocks (e.g. Mason et al 2007; Santelli
424 et al 2008; Mason et al., 2009; Lee et al., 2015), sulfide and carbonate hydrothermal deposits (e.g.
425 Sylvan et al., 2012; Kato et al., 2015), and giant foraminifera (Hori et al., 2013; Table 3b and Figure 5).
426 There are currently no cultivated representatives and metabolic information for these members of the
427 Bacteria, and it is not known whether they have metal tolerance mechanisms or they are actively
428 involved in metal cycling. The high abundance of potential metal reductive (i.e. Magnetospiraceae) and
429 oxidizers (i.e. Hyphomicrobiaceae), and presence of encrusting protozoans (Gooday et al., 2015),
430 microbial eukaryotes (Shulse et al., 2016) and metazoans (Vanreusel et al., 2016) create specific
431 ecological niches, which may be at least partially responsible for the observed selection of microbial
432 taxa in nodules. Overall, these findings suggest that bacterial groups adapted to lithic or biological
433 substrates preferentially colonize nodules, likely favoured by manganese and iron availability,
434 formation of biofilms and presence of sessile fauna communities.

435 The reduction and dissolution of Mn oxides by dissolved organic matter (e.g. humic compounds)
436 occurs typically in photic or reducing aquatic environments (Sunda et al., 1983; Stone and Morgan,
437 1984; Stone, 1987; Sunda and Huntsman, 1994). However reductive dissolution of Mn oxides by
438 dissolved organic substrates has been observed also in dark oxygenated seawater (Sunda et al., 1983;
439 Sunda and Huntsman, 1994), suggesting that it could be a relevant abiotic process in manganese
440 nodules. Indeed, this reaction yields manganese(II) and low-molecular-weight organic compounds
441 (Sunda and Kieber, 1994), which potentially may favour Mn-oxidizing Bacteria and microbial
442 exploitation of refractory dissolved organic matter. Intense extracellular enzymatic activities have been
443 reported for seafloor-exposed basalts (Meyers et al., 2014), raising the question of whether the closely
444 related microbes associated with nodules might have comparable degradation rates. Furthermore,
445 nodules host diversified communities of suspension feeders such as serpulid tubeworms, sponges,
446 corals and crinoids (Vanreusel et al., 2016), which filter microbes and POC from the bottom water and
447 release DOM and catabolic metabolites (e.g. ammonia). Thus, nodules may act as hot spots of organic
448 carbon degradation. Albeit metabolic activity has never been quantified on nodules and sequence
449 abundances are lower, the increased abundance of nitrifiers in nodules compared to the sediments
450 reported for Pacific Nodule Province (Tully and Heidelberg, 2013; Shulse et al., 2016) and in this study
451 could indicate a high metabolic activity. Nitrifiers catalyse the oxidation of ammonia, a catabolic
452 product of heterotrophic metabolism, to nitrite and eventually to nitrate. In the CCZ the nitrifier
453 community was composed of archaeal ammonia-oxidizing *Nitrosopumilus*, which represented a large
454 portion of the microbial assemblages (up to 20 %), and a minor contribution of bacterial nitrite-
455 oxidizing *Nitrospira* (Tully and Heidelberg, 2013; Shulse et al., 2016). Peru Basin sediments and
456 nodules showed more diversified nitrifier communities, which are enriched by ammonia oxidizing
457 *AqSI* (1 %) and unclassified Nitrosomonadaceae (1 %) and by nitrite-oxidizing *Nitrospina* (4 %) and
458 *Nitrospira* (1 %; Figure 4, Table S3 and Table 3a). *Nitrospina* are not commonly reported for deep-sea

459 sediments, but they are the dominant nitrite oxidizers in the oceans (Luecker et al., 2013). They have
460 recently been reported as symbiont of deep-sea glass sponges (Tian et al., 2016), which also commonly
461 colonize FeMn nodules (Vanreusel et al., 2016). The Nitrospina-related OTUs detected in the nodules
462 showed only low similarity with pelagic *Nitrospina gracilis* and *Nitrospina*-like sequences found in
463 deep-sea glass sponge (sequence identity of 93 %), but were closely related with sequences recovered
464 from marine basalts (Mason et al., 2007; Santelli et al. 2008; Mason et al. 2009), suggesting nodules as
465 a native habitat.

466 **5 Conclusions**

467 The sediments of nodule fields in the Peru Basin host a specific microbial community of bacterial taxa
468 reported for organic carbon poor environments (i.e. Chloroflexi, Planctomycetes) and potentially
469 involved in metal-cycling (i.e. Magnetospiraceae, Hyphomicrobiaceae). Nodule communities were
470 distinct from sediments and showed a higher proportion of sequences from potential Mn-cycling
471 bacteria including bacterial taxa found in ocean crust, nodules and hydrothermal deposits. Our results
472 are in general agreement with previous studies in the CCZ, confirming that nodules provide a specific
473 ecological niche. However remarkable differences in microbial community composition (e.g. Mn-
474 cycling bacteria, nitrifiers) between the CCZ and the Peru Basin also show that environmental settings
475 (e.g. POC flux) and features of FeMn nodules (e.g. metal content, nodule attached fauna) may play a
476 significant role in structuring the nodule microbiome. Due to limitations in the available datasets and
477 methodological differences in the studies existing to date, findings are not yet conclusive and cannot be
478 generalized. However, they indicate that microbial community structure and function would be
479 impacted by nodule removal. Future studies need to look at these impacts in more detail and should
480 address regional differences, to determine the spatial turnover and its environmental drivers, and the
481 consequences regarding endemic types.

482 Furthermore, our results suggest that the removal of nodules, and potentially also the blanketing of
483 nodules with plume sediments resuspended during the mining operations may affect the cycling of
484 metal and other elements. Future work is needed to characterize metabolic activities on and in nodules,
485 and to understand factors and processes controlling nodule colonization. Specifically, restoration
486 experiments should take place to test whether artificial substrates favour the recovery of microbial and
487 fauna communities, and their related ecological functions.

488 **Data availability**

489 Raw sequences with removed primer sequences were deposited at the European Nucleotide Archive
490 (ENA) under accession number PRJEB30517 and PRJEB32680.

491 **Author contributions**

492 **A.B., F.J., F.W. and M.M.** conceived the study. **A.B., F.J., F.W. and T.R.W.** performed sampling
493 activities. **M.M.** compiled and analysed the data. **M.M.** wrote the paper with the contribution from all
494 Authors.

495 **Competing interest**

496 The authors declare that they have no conflict of interest.

497 **Special issue statement**

498 **Acknowledgements**

499 The Authors want to thank captain and crew of the SO242/1 and /2 expedition, and M. Alisch, J.
500 Bäger, J. Barz, A. Nordhausen, F. Schramm, R. Stiens and W. Stiens, (HGF-MPG Joint Research
501 Group on Deep Sea Ecology and Technology) for technical support. The Authors are also grateful to
502 Dr. H. Tegetmeyer for support with Illumina sequencing (CeBiTec laboratory; HGF-MPG Joint
503 Research Group on Deep Sea Ecology and Technology). Lastly, the Authors would like to thank the
504 Dr. Denise Akob, Dr. Beth N. Orcutt, Dr. Tim D'Angelo and an anonymous reviewer, which
505 comments and suggestions great helped in improving the quality of the manuscript.

506 This work was funded by the German Ministry of Research and Education (BMBF grant no.
507 03F0707A-G) as part of the MiningImpact project of the Joint Programming Initiative of Healthy and
508 Productive Seas and Oceans (JPIOceans). We acknowledge further financial support from the
509 Helmholtz Association (Alfred Wegener Institute Helmholtz Center for Polar and Marine Research,
510 Bremerhaven) and the Max Planck Society (MPG), as well as from the ERC Advanced Investigator
511 Grant ABYSS (294757) to AB for technology and sequencing. The research has also received funding
512 from the European Union Seventh Framework Program (FP7/2007- 2013) under the MIDAS project,
513 grant agreement number 603418.

514 **References**

515 Altschul, S. F., Gish, W., Miller, W., Myers, E.W. and Lipman, D. J.: Basic local alignment search
516 tool. *J. Mol. Biol.* 215:403–410, 1990.
517 Anderson, M. J.: A new method for non-parametric multivariate analysis of variance, *Austral Ecol.*,
518 26(1), 32–46, 2001.
519 Andrews, S.: FastQC: a quality control tool for high throughput sequence data.
520 <http://www.bioinformatics.babraham.ac.uk/projects/fastqc/> (2010).
521 Bienhold, C., Boetius, A. and Ramette, A.: The energy – diversity relationship of complex bacterial
522 communities in Arctic deep-sea sediments, *ISME J.*, 6, 724–732, doi:10.1038/ismej.2011.140,
523 2012.
524 Bienhold, C., Zinger, L., Boetius, A. and Ramette, A.: Diversity and Biogeography of Bathyal and
525 Abyssal Seafloor Bacteria, *PLoS One*, 11(1), 1–20, doi:10.1371/journal.pone.0148016, 2016.
526 Blöthe, M., Węgorzewski, A., Müller, C., Simon, F., Kuhn, T. and Schippers, A.: Manganese-Cycling
527 Microbial Communities Inside Deep-Sea Manganese Nodules, *Environ. Sci. Technol.*, 49(13),
528 7692–7700, doi:10.1021/es504930v, 2015.
529 Bolger, A. M., Lohse, M. and Usadel, B.: Trimmomatic: a flexible trimmer for Illumina sequence data,
530 *Bioinformatics*, 30(15), 2114–2120, doi:10.1093/bioinformatics/btu170, 2014.

531 Boltenkov, B. S.: Mechanisms of formation of deep-sea ferromanganese nodules: Mathematical
 532 modeling and experimental results, *Geochemistry Int.*, 50(2), 125–132,
 533 doi:10.1134/S001670291120044, 2012.

534 Chao, A., J. Gotelli, N., Hsieh, T. C., L. Sander, E., H. Ma, K., Colwell, R. and M. Ellison, A.:
 535 Rarefaction and extrapolation with Hill numbers: A framework for sampling and estimation in
 536 species diversity studies, *Ecol. Monogr.*, 84, 45–67, doi:10.1890/13-0133.1, 2014.

537 Chester, R. and Jickells, T.: *Marine Geochemistry*, 3rd ed Wiley-Blackwell, Oxford., 2012.

538 Church, M. J., Wear, E. K., Orcutt, B. N., Young, C. R. and Smith, J. M.: Taxonomic diversity of
 539 Bacteria and Archaea in the Clarion-Clipperton Zone of the North Pacific Ocean. *Annex V in Deep*
 540 *CCZ Biodiversity Synthesis Workshop*, Friday Harbor, Washington, USA, 1-4 October 2019.

541 Cleary, D. F. R., Becking, L. E., Voogd, N. J. De, Pires, A. C. C., Ana, R. M. P., Egas, C. and Gomes,
 542 N. C. M.: Habitat- and host-related variation in sponge bacterial symbiont communities in
 543 Indonesian waters, *FEMS Microbiol. Ecol.*, 85, 465–482, doi:10.1111/1574-6941.12135, 2013.

544 Crerar, D. A. and Barnes, H. L.: Deposition of deep-sea manganese nodules, *Geochim. Cosmochim.
 545 Acta*, 38(2), 279–300, doi:10.1016/0016-7037(74)90111-2, 1974.

546 Diepenbroek, M., Glöckner, F. O., Grobe, P., Güntsch, A., Huber, R., König-Ries, B., Kostadinov, I.,
 547 Nieschulze, J., Seeger, B., Tolksdorf, R. and Triebel, D.: Towards an Integrated Biodiversity and
 548 Ecological Research Data Management and Archiving Platform : The German Federation for the
 549 Curation of Biological Data (GFBio), *Inform.* 2014 – Big Data Komplexität meistern. GI-Edition
 550 *Lect. Notes Informatics - Proc.*, 1711–1724, 2014.

551 Du, Z., Wang, Z., Zhao, J.-X. and Chen, G.: *Woeseia oceanii* gen. nov., sp. nov., a novel
 552 chemoheterotrophic member of the order Chromatiales, and proposal of *Woeseiaceae* fam. nov, *Int.
 553 J. Syst. Evol. Microbiol.*, 66, doi:10.1099/ijsem.0.000683, 2015.

554 Durbin, A. M. and Teske, A.: Microbial diversity and stratification of South Pacific abyssal marine
 555 sediments, *Environ. Microbiol.*, 13(12), 3219–3234, doi:10.1111/j.1462-2920.2011.02544.x, 2011.

556 Fernandes, A. D., Reid, J. N. S., Macklaim, J. M., McMurrough, T. A., Edgell, D. R. and Gloor, G. B.:
 557 Unifying the analysis of high-throughput sequencing datasets: characterizing RNA-seq, 16S rRNA
 558 gene sequencing and selective growth experiments by compositional data analysis, *Microbiome*,
 559 2(1), 15, doi:10.1186/2049-2618-2-15, 2014.

560 Galac, M. R., Bosch, I., and Janies, D. A.: Bacterial communities of oceanic sea star (Asteroidea:
 561 Echinodermata) larvae. *Mar. Biol.* 163, 162, DOI 10.1007/s00227-016-2938-3, 2016.

562 Gerpe, D., Buján, N., Diéguez, A. L., Lasa, A. and Romalde, J. L.: *Kiloniella majae* sp. nov ., isolated
 563 from spider crab (*Maja brachydactyla*) and pullet carpet shell clam (*Venerupis pullastra*) ♀, *Syst.
 564 Appl. Microbiol.*, 40, 274–279, doi:10.1016/j.syapm.2017.05.002, 2017.

565 Gobet, A., Boetius, A. and Ramette, A.: Ecological coherence of diversity patterns derived from
 566 classical fingerprinting and Next Generation Sequencing techniques, *Environ. Microbiol.*, 16(9),
 567 2672–2681, doi:10.1111/1462-2920.12308, 2014.

568 Gooday, A. J., Goineau, A. and Voltski, I.: Abyssal foraminifera attached to polymetallic nodules from
 569 the eastern Clarion Clipperton Fracture Zone: a preliminary description and comparison with North
 570 Atlantic dropstone assemblages, *Mar. Biodivers.*, 45(3), 391–412, doi:10.1007/s12526-014-0301-9,
 571 2015.

572 Haeckel, M., Konig, I., Reich, V., Weber, M. E. and Suess, E.: Pore water profiles and numerical
 573 modelling of biogeochemical processes in Peru Basin deep-sea sediments. *Deep-Sea Res Pt II* 48,
 574 3713-3736, doi.org/10.1016/S0967-0645(01)00064-9, 2001.

575 Halbach, P., Friedrich, G. and von Stackelberg, U.: The manganese nodule belt of the Pacific Ocean.
 576 Enke, Stuttgart, p 254, 1988.

577 Hassenrück, C., Quast, C., Rapp, J., and Buttigieg, P.: Amplicon. GitHub repository,
 578 <https://github.com/chasseur/NGS/tree/master/AMPLICON>, 2016.

579 Hoffmann, K., Bienhold, C., Buttigieg, P. L., Knittel, K., Laso-Pérez, R., Rapp, J. Z., Boetius, A. and
 580 Offre, P.: Diversity and metabolism of *Woeseiales* bacteria, global members of deep-sea sediment
 581 communities. *The ISME Journal* 14, 1042-1056, doi.org/10.1038/s41396-020-0588-4, 2020.

582 Hori, S., Tsuchiya, M., Nishi, S., Arai, W. and Takami, H.: Active Bacterial Flora Surrounding
 583 Foraminifera (*Xenophyophorea*) Living on the Deep-Sea Floor, *Biosci. Biotechnol. Biochem.*,
 584 77(2), 381–384, doi:10.1271/bbb.120663, 2013.

585 Hsieh, T.C., Ma, K. H. and Chao, A. iNEXT: iNterpolation and EXTrapolation for species diversity. R
 586 package version 2.0.17 URL, 2018: <http://chao.stat.nthu.edu.tw/blog/software-download/>.

587 J. Müller, P., Hartmann, M. and Suess, E.: The chemical environment of pelagic sediments, in Halbach
 588 P, Friedrich G, von Stackelberg U (eds) *The manganese nodule belt of the Pacific ocean:
 589 geological, environment, nodule formation, and mining aspects*. Enke, Stuttgart, pp. 70–90., 1988.

590 Jacob, M., Soltwedel, T., Boetius, A. and Ramette, A.: Biogeography of Deep-Sea Benthic Bacteria at
591 Regional Scale (LTER HAUSGARTEN, Fram Strait, Arctic), *PLoS One*, 8(9), e72779 [online]
592 Available from: <https://doi.org/10.1371/journal.pone.0072779>, 2013.

593 Jacobson Meyers, M. E., Sylvan, J. B. and Edwards, K. J.: Extracellular enzyme activity and microbial
594 diversity measured on seafloor exposed basalts from Loihi seamount indicate the importance of
595 basalts to global biogeochemical cycling, *Appl. Environ. Microbiol.*, 80(16), 4854–4864,
596 doi:10.1128/AEM.01038-14, 2014.

597 Kato, S., Ikehata, K., Shibuya, T., Urabe, T., Ohkuma, M. and Yamagishi, A.: Potential for
598 biogeochemical cycling of sulfur, iron and carbon within massive sulfide deposits below the
599 seafloor, *Environ. Microbiol.*, 17(5), 1817–1835, doi:10.1111/1462-2920.12648, 2015.

600 Kerr, R. A.: Manganese Nodules Grow by Rain from Above, *Science* (80-.), 223(4636), 576 LP –
601 577, doi:10.1126/science.223.4636.576, 1984.

602 Klindworth, A., Pruesse, E., Schweer, T., Peplies, J., Quast, C., Horn, M. and Glöckner, F. O.:
603 Evaluation of general 16S ribosomal RNA gene PCR primers for classical and next-generation
604 sequencing-based diversity studies, *Nucleic Acids Res.*, 41(1), e1–e1, doi:10.1093/nar/gks808,
605 2012.

606 Kuhn, T., Wegorzewski, A., Rühlemann, C. and Vink, A.: Composition, Formation, and Occurrence of
607 Polymetallic Nodules, in Deep-Sea Mining: Resource Potential, Technical and Environmental
608 Considerations, edited by R. Sharma, pp. 23–63, Springer International Publishing, Cham., 2017.

609 Larsen, E. I., Sly, L. I. and Mcewan, A. G.: Manganese (II) adsorption and oxidation by whole cells
610 and a membrane fraction of *Pedomicrobium* sp. ACM 3067, *Arch. Microbiol.*, 171(4), 257–264,
611 1999.

612 Lee, M. D., Walworth, N. G., Sylvan, J. B., Edwards, K. J. and Orcutt, B. N.: Microbial Communities
613 on Seafloor Basalts at Dorado Outcrop Reflect Level of Alteration and Highlight Global Lithic
614 Clades, *Front. Microbiol.*, 6, 1470, doi:10.3389/fmicb.2015.01470, 2015.

615 Lindh, M. V., Maillet, B. M., Shulse, C. N., Gooday, A. J., Amon, D. J., Smith, C. R. and Church, M.
616 J.: From the surface to the deep-sea: Bacterial distributions across polymetallic nodule fields in the
617 clarion-clipperton zone of the Pacific Ocean, *Front. Microbiol.*, 8(SEP), 1–12,
618 doi:10.3389/fmicb.2017.01696, 2017.

619 Luecker, S., Nowka, B., Rattei, T., Speck, E. and Daims, H.: The Genome of *Nitrospina gracilis*
620 Illuminates the Metabolism and Evolution of the Major Marine Nitrite Oxidizer, *Front. Microbiol.*
621 , 4, 27 [online] Available from: <https://www.frontiersin.org/article/10.3389/fmicb.2013.00027>,
622 2013.

623 Mahé, F., Rognes, T., Quince, C., de Vargas, C. and Dunthorn, M.: Swarm: robust and fast clustering
624 method for amplicon-based studies, *PeerJ*, 2, e593, doi:10.7717/peerj.593, 2014.

625 Martens-Habbena, W., Berube, P., Urakawa, H., De la Torre, J. and Stahl, D.: Ammonia oxidation
626 kinetics determine niche separation of nitrifying Archaea and Bacteria, *Nature*, 461, 976–979,
627 doi:10.1038/nature08465, 2009.

628 Martin, M.: Cutadapt removes adapter sequences from high-throughput sequencing reads,
629 *EMBnet.journal*; Vol 17, No 1 Next Gener. Seq. Data Anal. - 10.14806/ej.17.1.200 [online]
630 Available from: <https://journal.embnet.org/index.php/embnetjournal/article/view/200>, 2011.

631 Mason, O. U., Di Meo-Savoie, C. A., Van Nostrand, J. D., Zhou, J., Fisk, M. R. and Giovannoni, S. J.:
632 Prokaryotic diversity, distribution, and insights into their role in biogeochemical cycling in marine
633 basalts, *ISME J.*, 3(2), 231–242, doi:10.1038/ismej.2008.92, 2009.

634 Mason, O. U., Stingl, U., Wilhelm, L. J., Moeseneder, M. M., Di Meo-Savoie, C. A., Fisk, M. R. and
635 Giovannoni, S. J.: The phylogeny of endolithic microbes associated with marine basalts, *Environ.*
636 *Microbiol.*, 9(10), 2539–2550, doi:10.1111/j.1462-2920.2007.01372.x, 2007.

637 Matsunaga, T.: Applications of bacterial magnets Magnet, *Trends Biotechnol.*, 9(March), 91–95, 1991.

638 Mewes, K., Mogollón, J. M., Picard, A., Rühlemann, C., Kuhn, T., Nöthen, K. and Kasten, S.: Impact
639 of depositional and biogeochemical processes on small scale variations in nodule abundance in the
640 Clarion - Clipperton Fracture Zone, *Deep Sea Res. Part I Oceanogr. Res. Pap.*, 91, 125–141,
641 doi:<https://doi.org/10.1016/j.dsr.2014.06.001>, 2014.

642 Miller, K. A., Thompson, K. F., Johnston, P. and Santillo, D.: An Overview of Seabed Mining
643 Including the Current State of Development, Environmental Impacts, and Knowledge Gaps, *Front.*
644 *Mar. Sci.*, 4(January 2018), doi:10.3389/fmars.2017.00418, 2018.

645 Murray, J. and Renard, A. F.: Report on deep sea deposits based on the specimens collected during the
646 voyage of H.M.S. Challenger in the years 1872 - 1876, *Rep. Sci. results Voyag. H.M.S. Chall. Dur.*
647 years 1873 - 1876, 1–688, doi:<https://doi.org/10.1594/PANGAEA.849018>, 1891.

648 Offre, P., Spang, A. and Schleper, C.: Archaea in biogeochemical cycles. *Annu. Rev. Microbiol.* 67,
649 437–457. doi: 10.1146/annurev-micro-092412-155614, 2013.

650 Oksanen, J., Blanchet, F. G., Kindt, R. et al.: vegan: Community Ecology Package. R package version
 651 2.3-0, 2015.

652 Peukert, A., Schoening, T., Alevizos, E., Köser, K., Kwasnitschka, T. and Greinert, J.: Understanding
 653 Mn-nodule distribution and evaluation of related deep-sea mining impacts using AUV-based
 654 hydroacoustic and optical data, *Biogeosciences*, 15(8), 2525–2549, doi:10.5194/bg-15-2525-2018,
 655 2018.

656 Pruesse, E., Peplies, J. and Glöckner, F. O.: SINA: Accurate high-throughput multiple sequence
 657 alignment of ribosomal RNA genes, *Bioinformatics*, 28(14), 1823–1829,
 658 doi:10.1093/bioinformatics/bts252, 2012.

659 Riemann, F.: Biological aspects of deep-sea manganese nodule formation, *Oceanol. acta*, 6(3), 303–
 660 311, 1983.

661 Ruff, S. E., Biddle, J. F., Teske, A. P., Knittel, K., Boetius, A. and Ramette, A.: Global dispersion and
 662 local diversification of the methane seep microbiome, *Proc. Natl. Acad. Sci.*, 112(13), 4015 LP –
 663 4020, doi:10.1073/pnas.1421865112, 2015.

664 Santelli, C. M., Orcutt, B. N., Banning, E., Bach, W., Moyer, C. L., Sogin, M. L., Staudigel, H. and
 665 Edwards, K. J.: Abundance and diversity of microbial life in ocean crust, *Nature*, 453(May), 5–9,
 666 doi:10.1038/nature06899, 2008.

667 Schauer, R., Bienhold, C., Ramette, A. and Harder, J.: Bacterial diversity and biogeography in deep-sea
 668 surface sediments of the South Atlantic Ocean, *ISME J.*, 4, 159–170, doi:10.1038/ismej.2009.106,
 669 2010.

670 Schüler, D. and Frankel, R.: Bacterial magnetosomes: Microbiology, biominerization and
 671 biotechnological applications, *Appl. Microbiol. Biotechnol.*, 52, 464–473,
 672 doi:10.1007/s002530051547, 1999.

673 Scott, J. J., Glazer, B. T. and Emerson, D.: Bringing microbial diversity into focus: high-resolution
 674 analysis of iron mats from the Lō’ihī Seamount, *Environ. Microbiol.*, 19(1), 301–316,
 675 doi:10.1111/1462-2920.13607, 2017.

676 Shulse, C. N., Maillot, B., Smith, C. R. and Church, M. J.: Polymetallic nodules, sediments, and deep
 677 waters in the equatorial North Pacific exhibit highly diverse and distinct bacterial, archaeal, and
 678 microeukaryotic communities, *Microbiologyopen*, 6(2), 1–16, doi:10.1002/mbo3.428, 2017.

679 Si, O., Yang, H., Hwang, C. Y., Kim, S., Choi, S., Kim, J., Jung, M., Kim, S., Roh, S. W. and Rhee, S.:
 680 *Kiloniella antarctica* sp. nov., isolated from a polynya of Amundsen Sea in Western Antarctic Sea,
 681 *Int. J. Syst. Evol. Microbiol.*, 67, 2397–2402, doi:10.1099/ijsem.0.001968, 2017.

682 Simon-Lledo, E., Bett, B. J., Huvenne, V. A. I., Köser, K., Schoening, T., Greinert, J., and Jones, D. O.
 683 B.: Biological effects 26 years after simulated deep-sea mining. *Sci. Rep.* 9, 8040,
 684 doi:10.1038/s41598-019-44492-w, 2019.

685 Staudigel, H., Furnes, H., McLoughlin, N., Banerjee, N. R., Connell, L. B. and Templeton, A.: 3.5
 686 billion years of glass bioalteration: Volcanic rocks as a basis for microbial life?, *Earth-Science
 687 Rev.*, 89(3), 156–176, doi:https://doi.org/10.1016/j.earscirev.2008.04.005, 2008.

688 Stein, L. Y., Duc, M. T. La, Grundl, T. J. and Nealson, K. H.: Bacterial and archaeal populations
 689 associated with freshwater ferromanganese micronodules and sediments, *Environ. Microbiol.*, 3(1),
 690 10–18, 2001.

691 Sylvan, J. B., Toner, B. M. and Edwards, K. J.: Life and Death of Deep-Sea Vents: Bacterial Diversity
 692 and Ecosystem Succession on Inactive Hydrothermal Sulfides, edited by M. A. Moran, *MBio*, 3(1),
 693 e00279-11, doi:10.1128/mBio.00279-11, 2012.

694 Thiel, H., Schriever, G., Ahnert, A., Bluhm, H., Borowski, C. and Vopel, K.: The large-scale
 695 environmental impact experiment DISCOL - Reflection and foresight, *Deep. Res. Part II Top. Stud.
 696 Oceanogr.*, 48(17–18), 3869–3882, doi:10.1016/S0967-0645(01)00071-6, 2001.

697 Tian, R.-M., Sun, J., Cai, L., Zhang, W.-P., Zhou, G., Qui, J.-W. and Qian, P.-Y.: The deep - sea glass
 698 sponge *Lophophysema eversa* harbours potential symbionts responsible for the nutrient conversions
 699 of carbon, nitrogen and sulfur, *Environ. Microbiol.*, 18(8), 2481–2494, doi:10.1111/1462-
 700 2920.12911, 2016.

701 Tully, B. J. and Heidelberg, J. F.: Microbial communities associated with ferromanganese nodules and
 702 the surrounding sediments, *Front. Microbiol.*, 4(JUN), 1–10, doi:10.3389/fmicb.2013.00161, 2013.

703 Tyler, P. A.: Hyphomicrobia and the oxidation of manganese in aquatic ecosystems Mg /, *Antonie von
 704 Leeuwenhoek*, 36, 567–578, 1970.

705 Van den Boogaart, K. G., Tolosana, R. and Bren, M.: compositions: Compositional Data Analysis. R
 706 package version 1.40-1, 2014.

707 Vanreusel, A., Hilario, A., Ribeiro, P. A., Menot, L. and Arbizu, P. M.: Threatened by mining,
 708 polymetallic nodules are required to preserve abyssal epifauna, *Sci. Rep.*, 6, 26808 [online]
 709 Available from: <https://doi.org/10.1038/srep26808>, 2016.

710 Varliero, G., Bienhold, C., Schmid, F., Boetius, A. and Molari, M.: Microbial Diversity and
 711 Connectivity in Deep-Sea Sediments of the South Atlantic Polar Front, *Front. Microbiol.*, 10, 1–18,
 712 doi:10.3389/fmicb.2019.00665, 2019.

713 Volz, J. B., Mogollón, J. M., Geibert, W., Arbizu, P. M., Koschinsky, A. and Kasten, S.: Natural spatial
 714 variability of depositional conditions, biogeochemical processes and element fluxes in sediments of
 715 the eastern Clarion-Clipperton Zone, Pacific Ocean, *Deep. Res. Part I Oceanogr. Res. Pap.*,
 716 140(December 2017), 159–172, doi:10.1016/j.dsr.2018.08.006, 2018.

717 Von Stackelberg, U.: Growth history of manganese nodules and crusts of the Peru Basin, *Geol. Soc.*
 718 *London, Spec. Publ.*, 119(1), 153 LP – 176, doi:10.1144/GSL.SP.1997.119.01.11, 1997.

719 Vonnahme, T. R., Molari, M., Janssen, F., Wenzhöfer, F., Haeckel, M., Titschack, J. and Boetius, A.:
 720 Effects of a deep-sea mining experiment on seafloor microbial communities and functions after 26
 721 years. *Science Advances*, in press.

722 Walsh, E. A., Kirkpatrick, J. B., Rutherford, S. D., Smith, D. C., Sogin, M. and Hondt, S. D.: Bacterial
 723 diversity and community composition from seafloor to subseafloor, *ISME J.*, 10, 979–989,
 724 doi:10.1038/ismej.2015.175, 2016.

725 Wang, C., Liao, L., Xu, H., Xu, X., Wu, M. and Zhu, L.: Bacterial Diversity in the Sediment from
 726 Polymetallic Nodule Fields of the Clarion-Clipperton Fracture Zone, *J. Microbiol.*, 48(5), 573–585,
 727 doi:10.1007/s12275-010-0151-5, 2010.

728 Wang, L., Li, X., Lai, Q. and Shao, Z.: *Kiloniella litopenaei* sp. nov., isolated from the gut microflora
 729 of Pacific white shrimp, *Litopenaeus vannamei*, *Antonie Van Leeuwenhoek*, 108, 1293–1299,
 730 doi:10.1007/s10482-015-0581-5, 2015.

731 Wang, L., Yu, M., Liu, Y., Liu, J., Wu, Y., Li, L., Liu, J., Wang, M. and Zhang, X.-H.: Comparative
 732 analyses of the bacterial community of hydrothermal deposits and seafloor sediments across
 733 Okinawa Trough, *J. Mar. Syst.*, 180, 162–172, doi:<https://doi.org/10.1016/j.jmarsys.2016.11.012>,
 734 2018.

735 Wang, X. H., Gan, L. and Müller, W. E. G.: Contribution of biomineralization during growth of
 736 polymetallic nodules and ferromanganese crusts from the Pacific Ocean, *Front. Mater. Sci. China*,
 737 3(2), 109–123, doi:10.1007/s11706-009-0033-0, 2009.

738 Wang, Y. and Qian, P.-Y.: Conservative Fragments in Bacterial 16S rRNA Genes and Primer Design
 739 for 16S Ribosomal DNA Amplicons in Metagenomic Studies, *PLoS One*, 4(10), e7401 [online]
 740 Available from: <https://doi.org/10.1371/journal.pone.0007401>, 2009.

741 Wegorzewski, A. V. and Kuhn, T.: The influence of suboxic diagenesis on the formation of manganese
 742 nodules in the Clarion Clipperton nodule belt of the Pacific Ocean, *Mar. Geol.*, 357, 123–138,
 743 doi:10.1016/j.margeo.2014.07.004, 2014.

744 Wegorzewski, A. V., Kuhn, T., Dohrmann, R., Wirth, R. and Grangeon, S.: Mineralogical
 745 characterization of individual growth structures of Mn-nodules with different Ni+Cu content from
 746 the central Pacific Ocean, *Am. Mineral.*, 100(11–12), 2497–2508, doi:10.2138/am-2015-5122,
 747 2015.

748 Wiese, J., Thiel, V., Ga, A., Schmaljohann, R. and Imhoff, J. F.: alphaproteobacterium from the marine
 749 macroalga *Laminaria saccharina*, *Int. J. Syst. Evol. Microbiol.*, 59, 350–356,
 750 doi:10.1099/ij.s.0.001651-0, 2009.

751 Wu, Y. H., Liao, L., Wang, C. S., Ma, W. L., Meng, F. X., Wu, M. and Xu, X. W.: A comparison of
 752 microbial communities in deep-sea polymetallic nodules and the surrounding sediments in the
 753 Pacific Ocean, *Deep. Res. Part I Oceanogr. Res. Pap.*, 79, 40–49, doi:10.1016/j.dsr.2013.05.004,
 754 2013.

755 Xu, M., Wang, F., Meng, J. and Xiao, X.: Construction and preliminary analysis of a metagenomic
 756 library from a deep-sea sediment of east Pacific Nodule Province, *FEMS Microbiol. Ecol.*, 62(3),
 757 233–241, doi:10.1111/j.1574-6941.2007.00377.x, 2007.

758 Yang, S., Seo, H., Lee, J., Kim, S. and Kwon, K. K.: *Kiloniella spongiae* sp. nov., isolated from a
 759 marine sponge and emended description of the genus *Kiloniella* Wiese et al. 2009 and *Kiloniella*
 760 *laminariae*, *Int. J. Syst. Evol. Microbiol.*, 65, 230–234, doi:10.1099/ij.s.0.069773-0, 2015.

761 Zhang, G., He, J., Liu, F. and Zhang, L.: Iron-Manganese Nodules Harbor Lower Bacterial Diversity
 762 and Greater Proportions of Proteobacteria Compared to Bulk Soils in Four Locations Spanning
 763 from North to South China, *Geomicrobiol. J.*, 31(7), 562–577, doi:10.1080/01490451.2013.854428,
 764 2014.

765 Zhang, J., Kobert, K., Flouri, T. and Stamatakis, A.: PEAR: a fast and accurate Illumina Paired-End
 766 reAd mergeR, *Bioinformatics*, 30(5), 614–620, doi:10.1093/bioinformatics/btt593, 2013.

767 **Figure captions**

768 Figure 1. Comparison of diversity indices and unique OTUs between manganese nodules and
769 sediments for (a) bacterial and (b) archaeal communities. H_0 : number of OTUs ($q=0$); H_1 : exponential
770 Shannon ($q=1$); H_2 : inverse Simpson ($q=2$); Unique: OTUs present exclusively in each station
771 (percentage relative to total OTUs of whole dataset). Chao1 and Unique OTUs were calculated with
772 100 sequence re-samplings per sample to the smallest dataset (40613 sequences for Bacteria and 1835
773 sequences for Archaea). Red line shows the median. F : statistic *F-ratio*, with subscript numbers
774 reporting the degrees of freedom between groups and within groups, respectively; p : probability level;
775 KW-test: Kruskal-Wallis test; χ^2 : Chi square test value, with subscript numbers reporting the degrees
776 of freedom between groups and sample size, respectively.

777 Figure 2. Non-metric multidimensional scaling (NMDS) plot based on Euclidean distance similarity
778 matrix of bacterial (a) and archaeal (b) community structure at OTU level. Sequence abundances of
779 OTUs were centre log-ratio transformed. Permutational multivariate analysis of variance
780 (PERMANOVA) showed significant differences between nodule and sediment associated microbial
781 communities (for details see Table S1). Each sample (dot) is connected to the weighted averaged mean
782 of the within group distances. Ellipses represent one SD of the weighted averaged mean.

783 Figure 3. Bacterial community structure at dominant class level (cut-off $\geq 1\%$). MN: manganese
784 nodules; MUC: sediments.

785 Figure 4. Genera highly abundant in nodules (ALDEx2: glm adjusted $p < 0.01$; KW adjusted $p < 0.05$).
786 Base 2 logarithm of the ratios between geometric mean centred sequences number of nodule (Nod) and
787 sediment (Sed), and average of the sequences contribution of total number of sequences (%) retrieved
788 in nodules and in sediments are shown. For details see Table S3.

789 Figure 5. Habitats coverage for the closest related sequences ($\geq 99\%$ similarity) to OTUs highly
790 abundant in the nodules. For details see Table 4a-b.

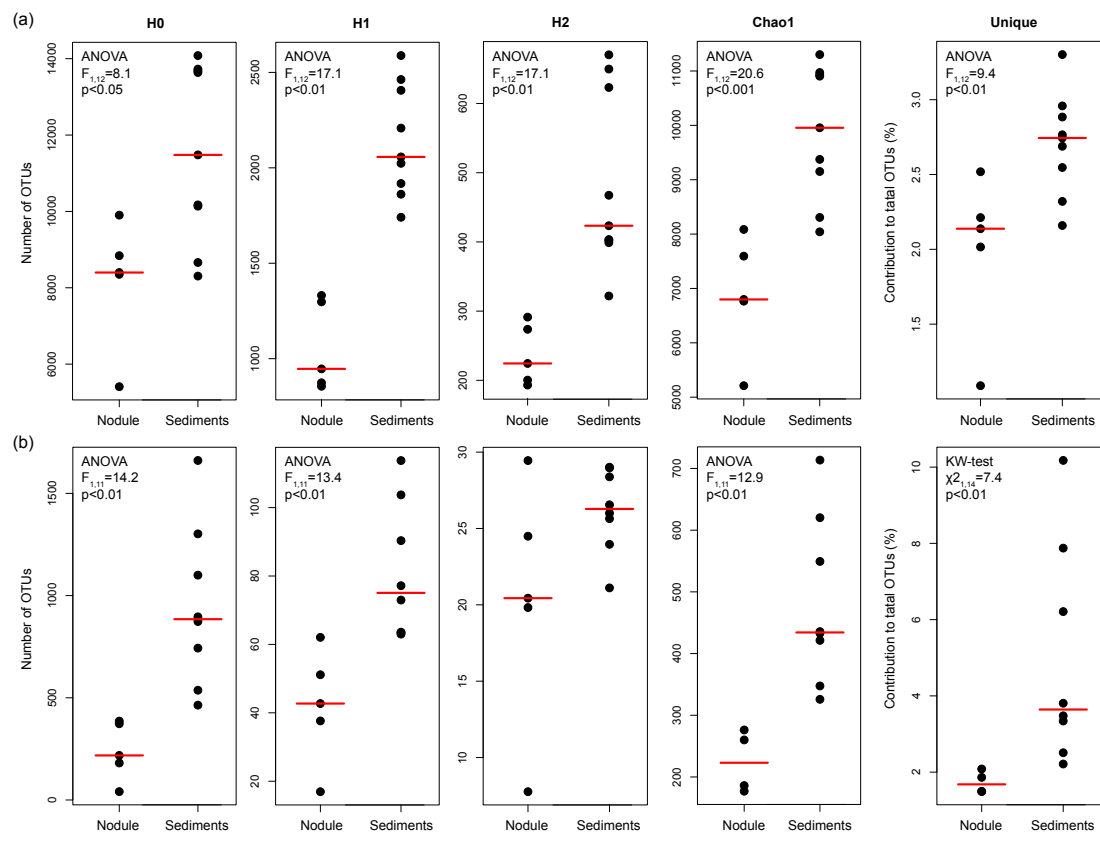
791 **Table captions**

792 Table 1. Stations list and description of investigated sites/substrates.

793 Table 2. Bacterial and archaeal diversity indices and unique OTUs for all nodules and sediment
794 samples. Indices and unique OTUs were calculated without singletons.

795 Table 3. (a) OTUs highly abundant in nodules (ALDEx2: glm adjusted $p < 0.01$; KW adjusted $p < 0.05$).
796 Only OTUs $\geq 0.1\%$ are reported. Base 2 logarithm of the ratios between geometric mean centred
797 sequences number of nodule (Nod) and sediment (Sed), and average of the sequences contribution of
798 total number of sequences (%) retrieved in nodules and in sediments are shown. (b) Closest related
799 sequences as indemnified with BLASTn (NCBI nucleotide database 12/06/2019).

800

Figure 1.

804 **Figure 2.**

805
806

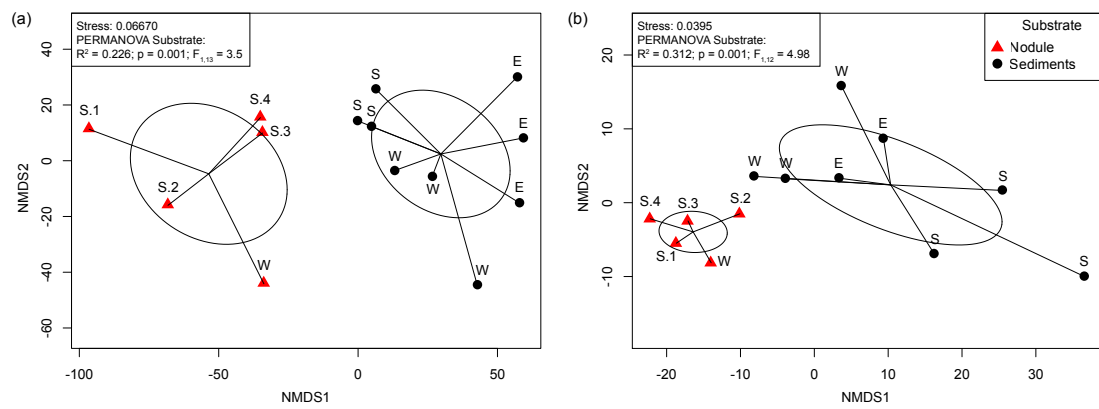
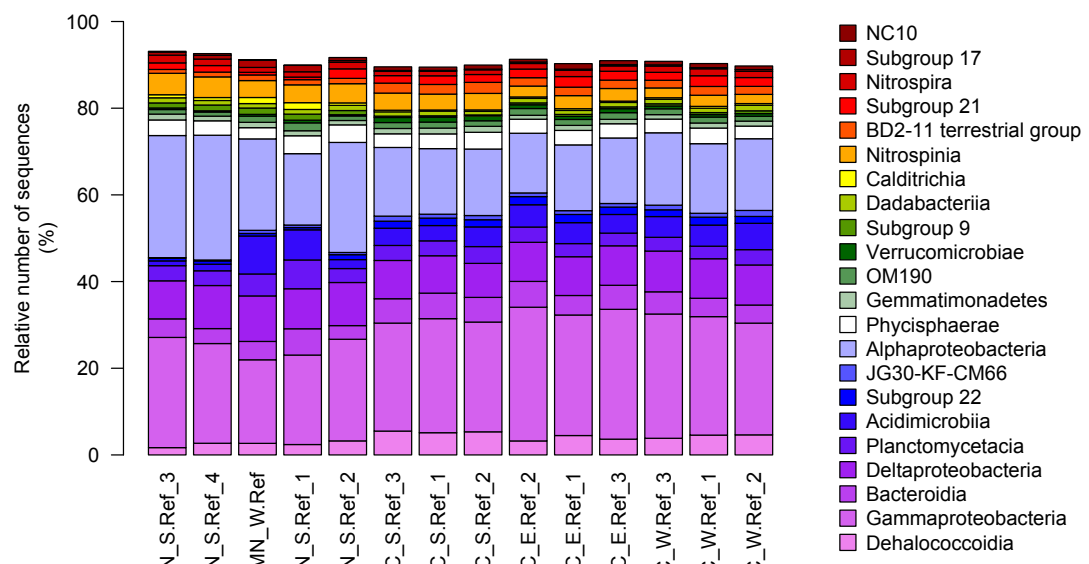
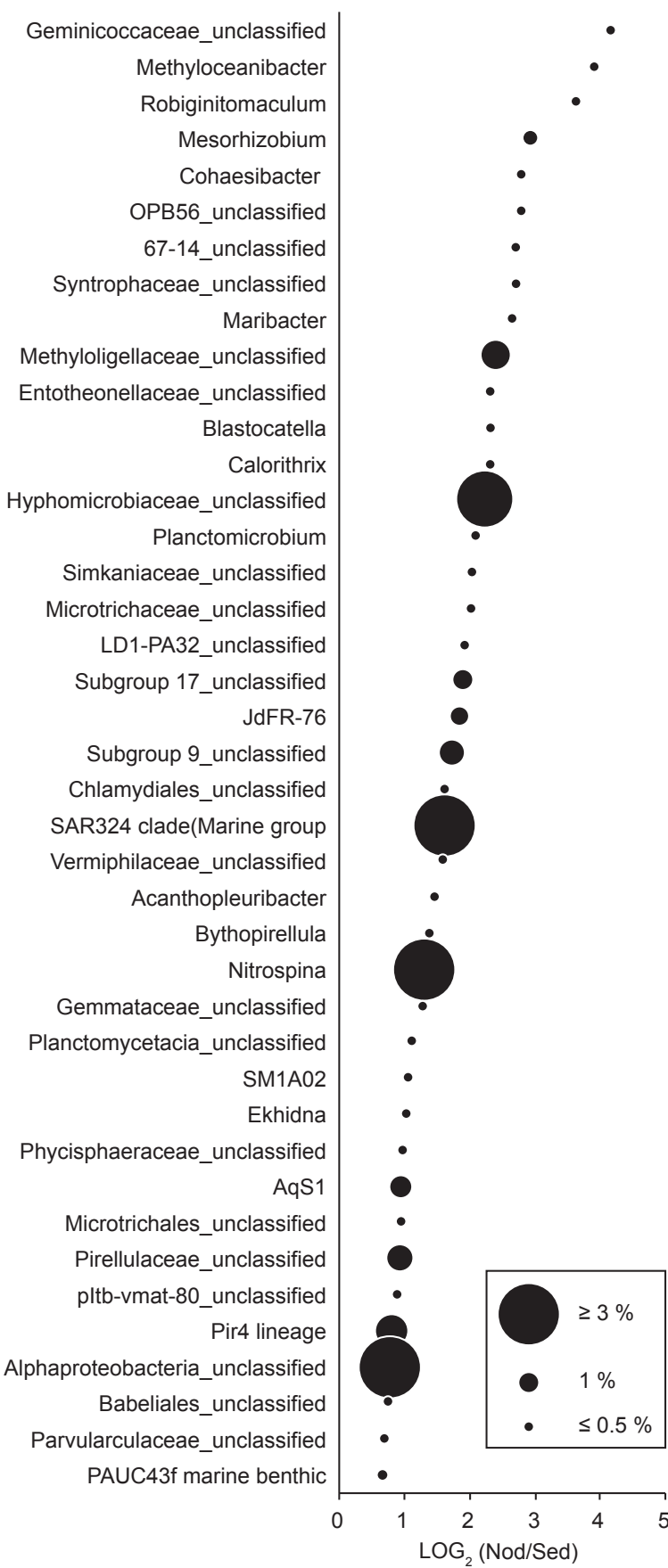
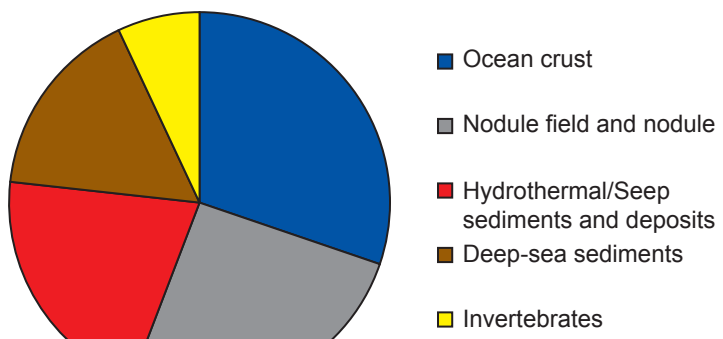


Figure 3.

809 **Figure 4.**



811 **Figure 5.**



812
813

Table 1.

Station	Sample ID	Sampling Time	Latitude (N)	Longitude (E)	Depth (m)	Device	Site	Sediment layer (cm bsf)	Substrate
SO242/2_147	MUC_E.Ref_1	02.09.15	-7.1007	-88.414	4198.2	MUC	Reference East	0-1	sediments
SO242/2_148	MUC_E.Ref_2	02.09.15	-7.1006	-88.414	4195.8	MUC	Reference East	0-1	sediments
SO242/2_151	MUC_E.Ref_3	03.09.15	-7.1006	-88.414	4197.8	MUC	Reference East	0-1	sediments
SO242/2_194	MN_W.Ref	15.09.15	-7.0761	-88.526	4129.5	MUC	Reference West	surface	nodule
SO242/2_194	MUC_W.Ref_1	15.09.15	-7.0761	-88.526	4129.5	MUC	Reference West	0-1	sediments
SO242/2_194	MUC_W.Ref_2	15.09.15	-7.0761	-88.526	4129.5	MUC	Reference West	0-1	sediments
SO242/2_194	MUC_W.Ref_3	15.09.15	-7.0761	-88.526	4129.5	MUC	Reference West	0-1	sediments
SO242/2_198	MN_S.Ref_1	16.09.15	-7.1262	-88.450	4145.6	ROV	Reference South	surface	nodule
SO242/2_198	MN_S.Ref_2	16.09.15	-7.1262	-88.450	4145.6	ROV	Reference South	surface	nodule
SO242/2_208	MN_S.Ref_3	19.09.15	-7.1256	-88.450	4150.7	MUC	Reference South	surface	nodule
SO242/2_208	MN_S.Ref_4	19.09.15	-7.1256	-88.450	4150.7	MUC	Reference South	surface	nodule
SO242/2_208	MUC_S.Ref_1	15.09.15	-7.0761	-88.526	4129.5	MUC	Reference South	0-1	sediments
SO242/2_208	MUC_S.Ref_2	15.09.15	-7.0761	-88.526	4129.5	MUC	Reference South	0-1	sediments
SO242/2_208	MUC_S.Ref_3	15.09.15	-7.0761	-88.526	4129.5	MUC	Reference South	0-1	sediments

815
816

MUC: TV-guided MUltiple Corer; ROV: Remote Operated Vehicle (Kiel 6000); bsf: below seafloor.

Table 2.

Bacteria	Sequences n. ^a	Sequences n. ^b	H ₀	H ₁	H ₂	Chao1 ^c	sd	Unique (%) ^c	sd
MUC_E.Ref_2	226078	161443	13638	2024	402	10930	201.6	2.7	0.1
MUC_E.Ref_3	218324	166847	13680	2057	423	10972	200.1	2.9	0.1
MUC_E.Ref_1	222924	164985	14082	2208	467	11302	166	3.0	0.1
MN_W.Ref	209563	159724	9902	1296	290	8085	143.6	2.2	0.1
MUC_W.Ref_1	137990	104301	11480	1918	403	9955	164	2.8	0.1
MUC_W.Ref_2	112259	81103	10171	1862	399	9151	148.3	2.3	0.1
MUC_W.Ref_3	236896	178985	13727	1741	322	10905	198.9	3.3	0.1
MN_S.Ref_1	313418	236498	8841	853	192	6798	138.3	2.5	0.1
MN_S.Ref_2	220364	172668	8399	872	199	6766	132.8	2.1	0.1
MN1_S.Ref_3	114074	43932	5409	945	223	5211	73.28	1.1	0.1
MN2_S.Ref_4	64218	76729	8351	1329	272	7594	124.2	2.0	0.1
MUC_S.Ref_1	77424	65890	10137	2588	670	9374	110.5	2.7	0.1
MUC_S.Ref_2	58575	45832	8662	2406	623	8306	93.85	2.2	0.1
MUC_S.Ref_3	59503	40613	8306	2463	650	8041	84.73	2.5	0.1

Archaea	Sequences n. ^d	Sequences n. ^b	H ₀	H ₁	H ₂	Chao1 ^c	sd	Unique (%) ^c	sd
MUC_E.Ref_2	40952	34494	896	63	21	433	52	3.5	0.5
MUC_E.Ref_3	25090	20215	743	73	26	421	50	3.3	0.6
MUC_E.Ref_1	na	na	na	na	na	na	na	na	na
MN_W.Ref	11737	12623	373	51	24	260	33	2.1	0.4
MUC_W.Ref_1	18097	14878	537	63	24	348	36	2.5	0.5
MUC_W.Ref_2	37656	31192	873	77	28	436	53	3.8	0.6
MUC_W.Ref_3	13031	10444	464	64	26	326	31	2.2	0.4
MN_S.Ref_1	7423	5384	218	38	20	186	26	1.5	0.3
MN_S.Ref_2	15314	9472	386	62	29	276	29	1.5	0.4
MN1_S.Ref_3	6099	1835	181	43	20	177	15	1.9	0.3
MN2_S.Ref_4 ^e	722	182	41	17	8	na	na	na	na
MUC_S.Ref_1	34166	29221	1100	90	27	549	66	6.2	0.6
MUC_S.Ref_2	41633	36378	1302	104	29	620	71	7.9	0.8
MUC_S.Ref_3	75344	64433	1661	114	29	714	75	10.2	0.9

819
820
821
822
823
824
825
826
827
828H₀: number of OTUs; H₁: exponential Shannon; H₂: inverse Simpson; Unique: OTUs present exclusively in one station (percentage relative to total OTUs of whole dataset); na: not available.^a after the merging of forward and reverse reads;^b after removal of un-specific and contaminants sequences (see Methods for details);^c calculated with 100 sequence re-samplings per sample to the smallest dataset (40613 sequences for Bacteria and 1835 sequences for Archaea), average data and standard deviation (sd) are given;^d after quality trimming of merged forward and reverse reads;^e due to extremely low number of sequences, this sample was not included in analyses requiring sequences re-sampling.

829 **Table 3.**

830 (a)

Phylum	Class	Order	Family	Genus	OTU	LOG2 (Nod/Sed)	Nodule (%)	Sediment (%)
Proteobacteria	Alphaproteobacteria	Rhizobiales	Hyphomicrobiaceae	Hyphomicrobiaceae_unclassified	otu29	2	2.5	0.7
Proteobacteria	Alphaproteobacteria	Rhodospirillales	Magnetospiraceae	Magnetospiraceae_unclassified	otu11	2	2.2	0.7
Proteobacteria	Alphaproteobacteria	Alphaproteobacteria_unclassified	Alphaproteobacteria_unclassified	Alphaproteobacteria_unclassified	otu31	8	1.5	0.0
Proteobacteria	Alphaproteobacteria	Alphaproteobacteria_unclassified	Alphaproteobacteria_unclassified	Alphaproteobacteria_unclassified	otu83	8	0.9	0.0
Proteobacteria	Alphaproteobacteria	Alphaproteobacteria_unclassified	Alphaproteobacteria_unclassified	Alphaproteobacteria_unclassified	otu160	6	0.3	0.0
Proteobacteria	Alphaproteobacteria	Alphaproteobacteria_unclassified	Alphaproteobacteria_unclassified	Alphaproteobacteria_unclassified	otu249	7	0.2	0.0
Proteobacteria	Delta proteobacteria	SAR324 clade(Marine group B)	SAR324 clade(Marine group B)_unclassified	SAR324 clade(Marine group B)_unclassified	otu66	8	0.7	0.0
Proteobacteria	Delta proteobacteria	SAR324 clade(Marine group B)	SAR324 clade(Marine group B)_unclassified	SAR324 clade(Marine group B)_unclassified	otu78	2	0.6	0.1
Proteobacteria	Delta proteobacteria	SAR324 clade(Marine group B)	SAR324 clade(Marine group B)_unclassified	SAR324 clade(Marine group B)_unclassified	otu202	3	0.4	0.0
Proteobacteria	Delta proteobacteria	SAR324 clade(Marine group B)	SAR324 clade(Marine group B)_unclassified	SAR324 clade(Marine group B)_unclassified	otu317	1	0.2	0.1
Proteobacteria	Delta proteobacteria	SAR324 clade(Marine group B)	SAR324 clade(Marine group B)_unclassified	SAR324 clade(Marine group B)_unclassified	otu947	4	0.2	0.0
Proteobacteria	Delta proteobacteria	SAR324 clade(Marine group B)	SAR324 clade(Marine group B)_unclassified	SAR324 clade(Marine group B)_unclassified	otu588	2	0.1	0.0
Proteobacteria	Delta proteobacteria	SAR324 clade(Marine group B)	SAR324 clade(Marine group B)_unclassified	SAR324 clade(Marine group B)_unclassified	otu425	2	0.1	0.0
Nitrospinae	Nitrospina	Nitrospinales	Nitrospinaeae	Nitrospina	otu68	3	1.4	0.1
Nitrospinae	Nitrospina	Nitrospinales	Nitrospinaeae	Nitrospina	otu227	6	0.2	0.0
Nitrospinae	Nitrospina	Nitrospinales	Nitrospinaeae	Nitrospina	otu215	3	0.2	0.0
Nitrospinae	Nitrospina	Nitrospinales	Nitrospinaeae	Nitrospira	otu636	6	0.2	0.0
Nitrospinae	Nitrospina	Nitrospinales	Nitrospinaeae	Nitrospira	otu434	3	0.1	0.0
Proteobacteria	Gammaproteobacteria	Arenicellales	Arenicellaceae	Arenicellaceae_unclassified	otu36	2	1.4	0.4
Proteobacteria	Gammaproteobacteria	Arenicellales	Arenicellaceae	Arenicellaceae_unclassified	otu162	5	0.4	0.0
Proteobacteria	Gammaproteobacteria	Steroidobacterales	Woesiaceae	Woesi	otu97	4	0.5	0.0
Proteobacteria	Gammaproteobacteria	Steroidobacterales	Woesiaceae	Woesi	otu266	2	0.2	0.1
Proteobacteria	Gammaproteobacteria	Steroidobacterales	Woesiaceae	Woesi	otu521	6	0.2	0.0
Proteobacteria	Gammaproteobacteria	Steroidobacterales	Woesiaceae	Woesi	otu346	4	0.2	0.0
Proteobacteria	Gammaproteobacteria	Steroidobacterales	Woesiaceae	Woesi	otu991	5	0.1	0.0
Proteobacteria	Alphaproteobacteria	Rhizobiales	Methyloligellaceae	Methyloligellaceae_unclassified	otu113	2	0.5	0.1
Proteobacteria	Alphaproteobacteria	Rhizobiales	Methyloligellaceae	Methyloligellaceae_unclassified	otu184	7	0.3	0.0
Proteobacteria	Alphaproteobacteria	Rhizobiales	Methyloligellaceae	Methyloligellaceae_unclassified	otu234	3	0.2	0.0
Acidobacteria	Subgroup 9	Subgroup 9_unclassified	Subgroup 9_unclassified	Subgroup 9_unclassified	otu255	6	0.5	0.0
Proteobacteria	Gammaproteobacteria	Nitrococcales	Nitrococcaceae	Aq51	otu122	2	0.8	0.3
Acidobacteria	Subgroup 17	Subgroup 17_unclassified	Subgroup 17_unclassified	Subgroup 17_unclassified	otu326	5	0.7	0.0
Acidobacteria	Subgroup 17	Subgroup 17_unclassified	Subgroup 17_unclassified	Subgroup 17_unclassified	otu865	1	0.1	0.1
Calditracheota	Calditrchia	Calditrchales	Calditrchaceae	JdFR-76	otu171	1	0.6	0.2
Calditracheota	Calditrchia	Calditrchales	Calditrchaceae	JdFR-76	otu541	4	0.2	0.0
Proteobacteria	Alphaproteobacteria	Rhodovibrionales	Kiloniellaceae	Kiloniellaceae_unclassified	otu357	3	0.1	0.0
Proteobacteria	Alphaproteobacteria	Rhodovibrionales	Kiloniellaceae	Kiloniellaceae_unclassified	otu435	4	0.1	0.0
Proteobacteria	Alphaproteobacteria	Rhodovibrionales	Kiloniellaceae	Kiloniellaceae_unclassified	otu370	3	0.1	0.0
Proteobacteria	Alphaproteobacteria	Rhodovibrionales	Kiloniellaceae	Kiloniellaceae_unclassified	otu467	6	0.1	0.0
Proteobacteria	Alphaproteobacteria	Rhodovibrionales	Kiloniellaceae	Kiloniellaceae_unclassified	otu450	2	0.1	0.0
Proteobacteria	Alphaproteobacteria	Rhizobiales	Kiloniellaceae	Kiloniellaceae_unclassified	otu519	3	0.1	0.0
Proteobacteria	Alphaproteobacteria	Rhizobiales	Kiloniellaceae	Cohaesibacter	otu71	4	0.7	0.1
Actinobacteria	Acidimicrobia	Actinominales	Actinominales_unclassified	Actinominales_unclassified	otu163	2	0.3	0.1
Actinobacteria	Acidimicrobia	Actinominales	Actinominales_unclassified	Actinominales_unclassified	otu532	6	0.2	0.0
Acidobacteria	Subgroup 9	Subgroup 9_unclassified	Subgroup 9_unclassified	Subgroup 9_unclassified	otu342	3	0.3	0.0
Acidobacteria	Subgroup 9	Subgroup 9_unclassified	Subgroup 9_unclassified	Subgroup 9_unclassified	otu674	3	0.1	0.0
Gemmimonadetes	Gemmimonadetes	Gemmimonadetes	Gemmimonadaceae	Gemmimonadaceae_unclassified	otu203	1	0.4	0.2
Proteobacteria	Alphaproteobacteria	Kordimonadales	Kordimonadaceae	Kordimonas	otu86	2	0.4	0.1
Bacteroidetes	Bacteroidia	Cytophagales	Cyclobacteriaceae	Cyclobacteriaceae_unclassified	otu233	3	0.4	0.0
Dababacteria	Dababacteria	Dababacterales	Dababacteriales_unclassified	Dababacteriales_unclassified	otu347	3	0.2	0.0
Dababacteria	Dababacteria	Dababacterales	Dababacteriales_unclassified	Dababacteriales_unclassified	otu1016	3	0.1	0.0
Actinobacteria	Thermoleophilia	Solirubrobacterales	67-14	67-14_unclassified	otu324	3	0.3	0.0
Proteobacteria	Delta proteobacteria	NB1-j	NB1-j_unclassified	NB1-j_unclassified	otu344	1	0.1	0.0
Planctomycetes	Planctomycetacia	Pirellulales	Pirellulaceae	Pirellulaceae_unclassified	otu538	2	0.1	0.0
Actinobacteria	Acidimicrobia	Microtrichales	Microtrichaceae	Microtrichaceae_unclassified	otu669	2	0.1	0.0
Acidobacteria	Blastocatelia (Subgroup 4)	Blastocatellales	Blastocatellaceae	Blastocatella	otu489	3	0.1	0.0
Entotheneellaeota	Entotheneellia	Entotheneellales	Entotheneellaceae	Entotheneellaceae_unclassified	otu788	4	0.1	0.0
Acidobacteria	Thermoanaerobaculia	Thermoanaerobaculales	Thermoanaerobaculaceae	Subgroup 10	otu711	3	0.1	0.0
Proteobacteria	Gammaproteobacteria	Oceanospirillales	Kangiellaceae	Kangiellaceae_unclassified	otu744	5	0.1	0.0
Proteobacteria	Gammaproteobacteria	Thiohalorhabdales	Thiohalorhabdaceae	Thiohalorhabdaceae_unclassified	otu571	6	0.1	0.0
Bacteroidetes	Bacteroidia	Cytophagales	Cyclobacteriaceae	Ekhidna	otu651	5	0.1	0.0
Bacteroidetes	Bacteroidia	Flavobacteriales	Flavobacteriaceae	Flavobacteriaceae_unclassified	otu579	6	0.1	0.0
Gemmimonadetes	BD2-11 terrestrial group	BD2-11 terrestrial group_unclassified	BD2-11 terrestrial group_unclassified	BD2-11 terrestrial group_unclassified	otu1439	3	0.1	0.0

831

832 (b)

OTU	NCBI ID \geq 99% similarity	Habitat(s)
otu29	KT748605.1; JX227334.1; EU491654.1	basaltic crust; nodule fields
otu11	JX227511.1; JQ013353.1; FJ938664.1	nodule fields; deep-sea sediments; cobalt-rich crust
otu31	MG580220.1; KF268757.1	Mariana subduction zone sediments; heavy metal contaminated marine sediments
otu83	MG580220.1; JN621543.1	Mariana subduction zone sediments; manganese oxide-rich marine sediments
otu160	MG580740.1; JX227257.1	Mariana subduction zone sediments; nodule fields
otu249	JQ287236.1; KM051824.1	inactive hydrothermal sulfides; basaltic crust
otu66	JX226721.1 ^a	nodule fields
otu78	JN860354.1; HQ721444.1	hydrothermal vents; deep-sea sediments;
otu202	MG580143.1; JX227690.1; JN860358.1	Mariana subduction zone sediments; nodule fields; hydrothermal vents
otu317	JX227432.1; AY627518.1	nodule fields; deep-sea sediments;
otu947	JX226721.1 ^a	nodule fields
otu588	LC081043.1	nodule
otu425	JX227680.1; FJ938661.1	nodule fields; cobalt-rich crust
otu68	JN886931.1; FJ752931.1; KJ590663.1	hydrothermal carbonate sediments; polychaete burrow environment; biofilm
otu227	MG580382.1; AM997732.1	Mariana subduction zone sediments; deep-sea sediments
otu215	KC901562.1; AB015560.1	basaltic glasses; deep-sea sediments
otu636	HM101002.1; EU491612.1; KC682687.1	Marine Sponge Halichondria; ocean crust;
otu434	EU287401.1; JN977323.1	Subsurface sediments; marine sediments
otu36	JX227383.1; KY977840.1; AM997938.1	nodule fields; Mariana subduction zone sediments; deep-sea sediments
otu162	FN553503.1; AM997671.1	hydrothermal vents; deep-sea sediments
otu97	JX227693.1; FJ024322.1; EU491736.1	nodule fields; ocean crust
otu266	AB694157.1; JX227083.1	deep-sea benthic foraminifera; nodule fields
otu521	KY977757.1; KT336088.1; JX227223.1	Mariana subduction zone sediments; nodules; nodule fields
otu346	KY977757.1; JX227223.1	Mariana subduction zone sediments; nodule fields
otu991	JX227363.1; AM997733.1	nodule fields; deep-sea sediments
otu113	JX226757.1; EU491557.1	nodule fields; ocean crust
otu184	EU491404.1	ocean crust
otu234	EU491604.1	ocean crust
otu255	JX227709.1; FJ437705.1; KM110219.1	nodule fields; hydrothermal deposits
otu122	MG580277.1; AM997814.1; AJ966605.1	Mariana subduction zone sediments; deep-sea sediments; nodule fields
otu326	JN886905.1; KT748584.1	hydrothermal carbonate sediments; basalt crust
otu865	JX227375.1; FJ938651.1; AY225640.1	nodule fields; cobalt-rich crust; hydrothermal sediments
otu171	AM997407.1; FJ205352.1; EU491267.1	deep-sea sediments; hydrothermal vents; ocean crust
otu541	AB694393.1	deep-sea benthic foraminifera
otu357	EU236317.1; GU302472.1	marine sponge; hydrocarbon seep
otu435	KY609381.1; KM051717.1; JX226899.1	Fe-rich hydrothermal deposits; basaltic crust; nodule fields
otu370	EU491648.1 ^a	ocean crust
otu467	FN553612.1; AB858542.1; KM051770.1	hydrothermal vents; sulfide deposits; basaltic crust
otu450	AM997745.1; KM051762.1; EU491108.1	deep-sea sediments; basaltic crust; ocean crust
otu519	GU220747.1; MG580729.1	Fe-rich hydrothermal deposits; Mariana subduction zone sediments
otu71	FJ205181.1; JX226787.1	hydrothermal vents; noduel fields
otu163	JX227427.1; JN886907.1; EU491661.1	nodule fields; hydrothermal carbonate sediments; ocean crust
otu532	EU491402.1; JX227188.1; EU374100.1	ocean crust; nodule fields; deep-sea sediments
otu342	JX227410.1; FJ205219.1; KT336055.1	nodule fields; hydrothermal vents; nodules
otu674	JX227662.1; KT336085.1; FJ938601.1	nodule fields; nodules; cobalt-rich crust
otu203	KP305065.1; FJ938598.1	corals; cobalt-rich crust
otu86	AM997620.1; FJ938474.1	deep-sea sediments; cobalt-rich crust
otu233	JX227464.1; AM997441.1	nodule fields; deep-sea sediments
otu347	JX227062.1; EU491655.1	nodule fields; ocean crust
otu1016	KF616695.1; KM396663.1; EU491261.1	carbonate methane seep; brine seep; ocean crust
otu324	JX226791.1; JN886912.1	nodule fields; hydrothermal carbonate sediments
otu344	EU438185.1; KY977824.1	deep-sea sediments and hydrothermal vents; ocean crust
otu538	KM356353.1; JX226930.1; DQ996924.1	carbonate methane seep; nodule fields; deep-sea sediments
otu669	EU491619.1; MG580068.1; KT748607.1	ocean crust
otu489	EU491660.1; MG580531.1; AM998023.1	ocean crust; deep-sea sediments
otu788	JN886890.1; MG580099.1	hydrothermal carbonate sediments; ocean crust
otu711	JX193423.1; GU302449.1; AY225643.1	mariculture sediments; hydrocarbon seep; ocean crust
otu744	AB831375.1; EU290406.1; KM454306.1	deep-sea methane-seep sediments; marine sponge; marine sediments
otu571	JQ287033.1; AM911385.1; EU236424.1	hydrothermal sulfides; cold-water corals; sponges
otu651	KT972875.1 ^a	outcrops
otu579	EU491573.1; KT336070.1	ocean crust; nodules
otu1439	JN886922.1; KC747092.1; JN884864.1	hydrothermal carbonate sediments; deep-sea sediments; methane seep